

Discovery of [1,2,4]triazolo[4,3-*a*]pyridines as potent Smoothed inhibitors targeting the Hedgehog pathway with improved antitumor activity in vivo

Nannan Tian, Huanxian Wu, Huiwu Zhang, Danni Yang, Lin Lv, Zichao Yang, Tingting Zhang, Dongling Quan, Lei Zhou, Ying Xie, Yimei Xu, Ning Wei, Jiajie Zhang, Mian Chen, John C. Schmitz, Yuanxin Tian, Shaoyu Wu

PII: S0968-0896(20)30414-4
DOI: <https://doi.org/10.1016/j.bmc.2020.115584>
Reference: BMC 115584



To appear in: *Bioorganic & Medicinal Chemistry*

Received Date: 15 April 2020
Revised Date: 28 May 2020
Accepted Date: 1 June 2020

Please cite this article as: Tian, N., Wu, H., Zhang, H., Yang, D., Lv, L., Yang, Z., Zhang, T., Quan, D., Zhou, L., Xie, Y., Xu, Y., Wei, N., Zhang, J., Chen, M., Schmitz, J.C., Tian, Y., Wu, S., Discovery of [1,2,4]triazolo[4,3-*a*]pyridines as potent Smoothed inhibitors targeting the Hedgehog pathway with improved antitumor activity in vivo, *Bioorganic & Medicinal Chemistry* (2020), doi: <https://doi.org/10.1016/j.bmc.2020.115584>

This is a PDF file of an article that has undergone enhancements after acceptance, such as the addition of a cover page and metadata, and formatting for readability, but it is not yet the definitive version of record. This version will undergo additional copyediting, typesetting and review before it is published in its final form, but we are providing this version to give early visibility of the article. Please note that, during the production process, errors may be discovered which could affect the content, and all legal disclaimers that apply to the journal pertain.

Discovery of [1,2,4]triazolo[4,3-a]pyridines as potent Smoothened inhibitors targeting the Hedgehog pathway with improved antitumor activity in vivo

Nannan Tian^{a,f,1}, Huanxian Wu^{a,1}, Huiwu Zhang^{a,1}, Danni Yang^a, Lin Lv^a, Zichao Yang^a, Tingting Zhang^a, Dongling Quan^a, Lei Zhou^a, Ying Xie^b, Yimei Xu^c, Ning Wei^d, Jiajie Zhang^a, Mian Chen^c, John C. Schmitz^{d,*}, Yuanxin Tian^{a,*}, Shaoyu Wu^{a,*}

^a Guangdong Provincial Key Laboratory of New Drug Screening, School of Pharmaceutical Science, Southern Medical University, Guangzhou, 510515, PR China;

^b State Key Laboratory for Quality Research of Chinese Medicines, Macau University of Science and Technology, Taipa, Macau, China;

^c The Center for Disease Control and Prevention of Xinjiang Uygur Autonomous Region, Urumqi Xinjiang, 830002, PR China;

^d Cancer Therapeutics Program, UPMC Hillman Cancer Center, University of Pittsburgh, Pittsburgh, PA, USA;

^e Oxford Transplant Centre, Churchill Hospital, Oxford University Hospitals NHS Foundation Trust, Old Road, Headington, Oxford, OX3 7LE, United Kingdom;

^f Key Laboratory of Orthopaedics and Traumatology, The First Affiliated Hospital of Guangzhou University of Chinese Medicine, The First Clinical Medical College, Guangzhou University of Chinese Medicine, Guangzhou, PR China.

Abbreviations: Hh, Hedgehog; Gli1, glioma-associated oncogene 1; Ptch, patched; Smo, Smoothened; ATO, Arsenic Trioxide; AML, Acute myeloid leukemia; TNBC, triple-negative breast cancer ; FDA, Food and Drug Administration; DIPEA, N,N-Diisopropylethylamine; SPR, surface plasmon resonance; MTT, 3-(4,5-dimethyl-2-thiazolyl)-2,5-diphenyl-2-H-tetrazolium bromide; Shh, Sonic Hedgehog; IC50, half-maximal inhibitory concentration; LD50, half-leathal dose; Ac-Tub, Acetylated α -tubulin; IFD, Induce-fit docking; PK, pharmacokinetics.

*Corresponding authors.

E-mail addresses: Shaoyu Wu (wushaoyu@smu.edu.cn), Yuanxin Tian(tyx523@smu.edu.cn), John C. Schmitz(schmitzjc@upmc.edu).

¹ These authors contributed equally to the work.

Abstract:

Triple-negative breast cancer (TNBC), a subset of breast cancers, have poorer survival than other breast cancer types. Recent studies have demonstrated that the abnormal Hedgehog (Hh) pathway is activated in TNBC and that these treatment-resistant cancers are sensitive to inhibition of the Hh pathway. Smoothened (Smo) protein is a vital constituent in Hh signaling and an attractive drug target. Vismodegib (VIS) is one of the most widely studied Smo inhibitors. But the clinical application of Smo inhibitors is limited to adult patients with BCC and AML, with many side effects. Therefore, it's necessary to develop novel Smo inhibitor with better profiles. Twenty [1,2,4]triazolo[4,3-a]pyridines were designed, synthesized and screened as Smo inhibitors. Four of these novel compounds showed directly bound to Smo protein with stronger binding affinity than VIS. The new compounds showed broad anti-proliferative activity against cancer cell lines in vitro, especially triple-negative breast cancer cells. Mechanistic studies demonstrated that **TPB15** markedly induced cell cycle arrest and apoptosis in MDA-MB-468 cells. **TPB15** blocked Smo translocation into the cilia and reduced Smo protein and mRNA expression. Furthermore, the expression of the downstream regulatory factor glioma-associated oncogene 1 (Gli1) was significantly inhibited. Finally, **TPB15** demonstrated greater anti-tumor activity in our animal models than VIS with lower toxicity. Hence, these results support further optimization of this novel scaffold to develop improved Smo antagonists.

Keywords: Hedgehog pathway; Smoothened inhibitor; triple-negative breast cancer

1. Introduction

Hedgehog signaling is necessary for the growth and formation of numerous tissues during embryogenesis, which is mostly quiescent in adults ¹. The main constituents of this pathway include the Hh ligands (Sonic, Desert, Indian), Patched receptor (Ptch), Smoothened receptor (Smo), and the terminal transcription factors Gli1-3, that regulate the transcription of Hh target genes ¹⁻³. When the Hh ligand binds to Ptch directly, the inhibition of Ptch on Smo is reduced, thus activating the Hh signaling pathway⁴. Subsequently, activated Smo translocates into the primary cilia, resulting in activation and nuclear accumulation of Gli, which regulates cell proliferation, survival and differentiation ^{4,5}. It had be reported that abnormal activation of Hh signaling is related to the progression of multiple cancers such as medulloblastoma, basal cell carcinoma (BCC), acute myeloid leukemia (AML), rhabdomyosarcoma, prostate, lung and breast cancers ^{1,4,6}. Smo, as a G protein-coupled receptor, is a vital constituent in Hh signaling pathway and an attractive drug target⁴. Smo gets more attention than other components of Hh signaling pathway because of its flexibility and feasibility^{7,8}.

The first Smo inhibitor Vismodegib (GDC-0449, **VIS**) was approved by the US Food and Drug Administration (FDA) in 2012 for the treatment of BCC patients ⁹. After that , many other Smo inhibitors have been come out, including the approved drugs Sonidegib (NVP-LDE225), Glasdegib (PF-04449913) and Patidegib (IPI-926) ¹⁰ (**Fig. 1**). ^{11,12}. Clinical trials of the Smo inhibitors demonstrated not only hopeful results in BCC patients, but also provided medical cures for patients cannot be treated with traditional surgery or radiotherapy^{13,14}. The abnormal activation of the Hh signaling pathway in the

initiation and development of various cancers urges the investigation of the Smo inhibitors in other cancers.

Despite significant results with Smo-targeted antagonists or other Hh signaling inhibitors, the clinical application of Smo inhibitors is limited to adult patients with BCC and AML, with many side effects, including diarrhea, constipation, loss of appetite, alopecia, muscle cramps, and fatigue. Therefore, more and more attention were paid on discovering novel inhibitors with better profiles.

Previous findings have shown that overexpression of the Hh pathway predicts poor outcome for breast cancer patients ¹⁵. Triple-negative breast cancer (TNBC), a subset of breast cancers, have poorer survival than other breast cancer types. Recent studies have demonstrated that the Hh pathway is activated in TNBC and that these treatment-resistant cancers are sensitive to inhibition of the Hh pathway ¹⁶⁻¹⁸. Early phase clinical trials have revealed antitumor activity of the Smo inhibitor Sonidegib in TNBC ^{19, 20}. Thus, the Hh pathway is a promising target for treatment of TNBC and development of novel Smo inhibitors with superior therapeutic properties is crucial for improved patient outcomes.

We designed and synthesized Twenty [1,2,4]triazolo[4,3-a]pyridines were as novel Smo inhibitors. Then screened the bioactivities of the novel compounds.

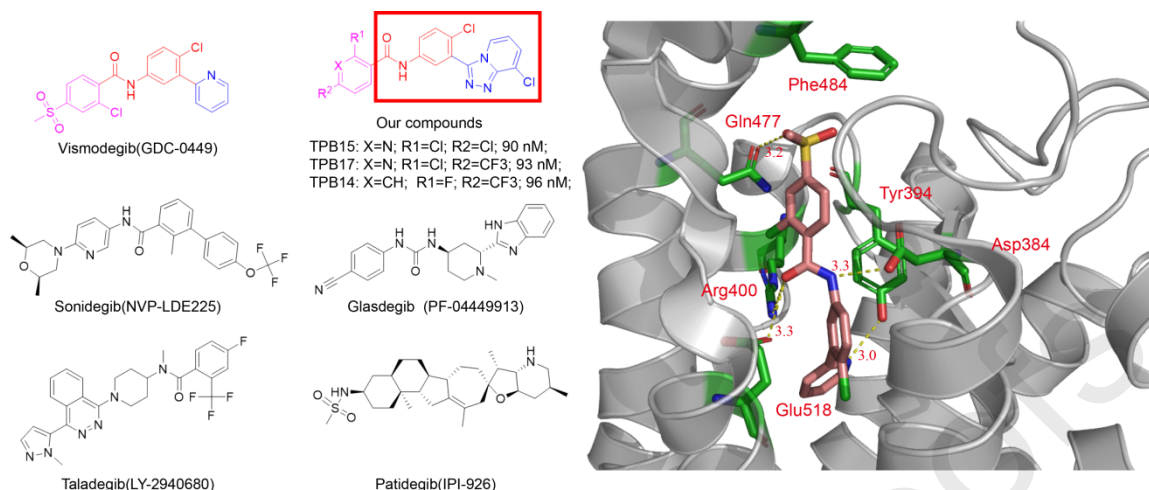


Fig. 1. Chemical structure of Smo inhibitors, our designed compounds, and the binding conformation of VIS to Smo protein. Yellow dot line represents the H-bonds, and the number on it is the distance of the H-bone.

2. Results and discussion

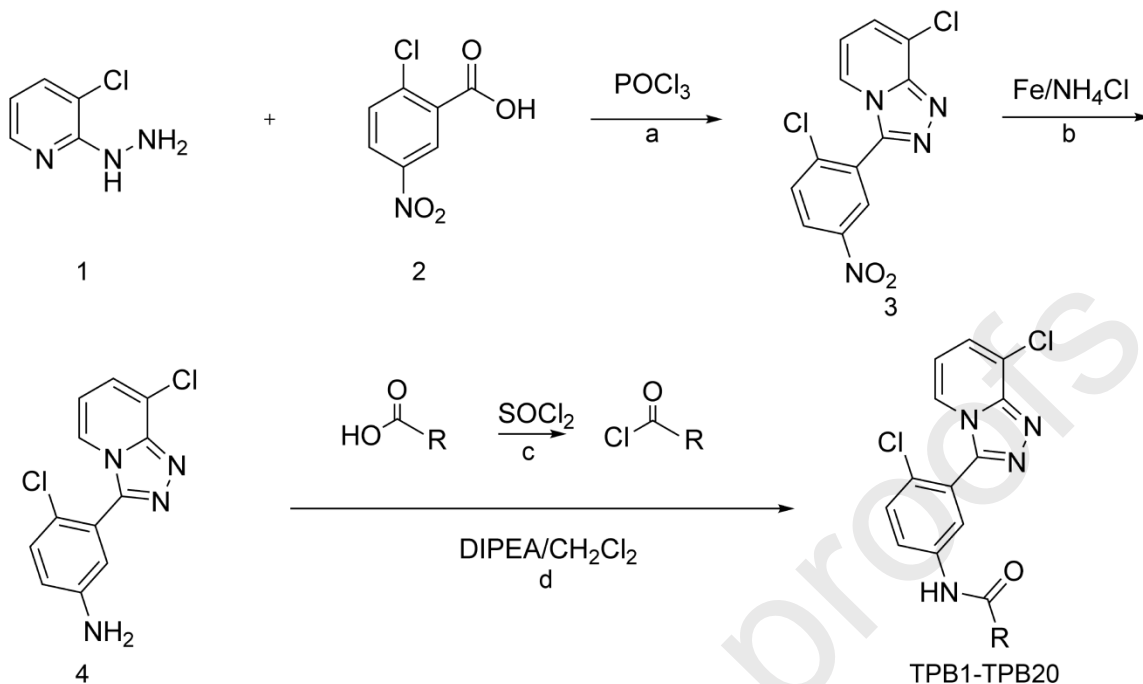
2.1. Analysis of Co-crystal complex of Vismodegib with Smo and design strategy

The co-crystal structures of human Smo receptor combined with VIS reported recently provided target structure and interaction details for structure-based drug discovery²¹. According to binding analysis based on the crystal structure, the VIS molecule can be divided into three parts (**Fig. 1**): the red part including the chloro-phenyl ring and amide linker, acts as the core skeleton of Smo protein targeting moiety. It can occupy the central hydrophobic pocket of the transmembrane domain. The H-bond formed with the Asp384 and the potential H-bonds with Arg400 can stabilize the conformation of VIS and play an important role in its binding affinities²¹. Based on chemical structure/binding conformation analysis, we designed novel Smo inhibitors for the treatment of Hh-dependent malignancies. Considering that triazole derivatives including pyridine derivatives show a wide range of biological activities (insecticidal,

anti-inflammatory, anti-tumor, microbicides and anti-bacterial and relaxing blood vessels^{22, 23}), we replaced the pyridyl of **VIS** (blue part; **Fig. 1**) with [1,2,4]triazolo[4,3-a]pyridine. As an electron-deficient group, it maintains the pi-pi interaction with the Ar ring within the target protein. The N atoms from the [1,2,4]triazolo[4,3-a]pyridine group are expected to form H-bonds with Smo protein (such as Tyr394) contributing to its antagonistic activity, similar to the role of pyridine in **VIS**. In order to further optimize compound activity, the chlorophenyl-methylsulfone moiety (magenta part; **Fig. 1**) was replaced with different five- or six-membered aromatic rings.

2.2. Chemistry

A series of [1,2,4]triazolo[4,3-a]pyridines were synthesized according to the process outlined in **Scheme 1**. 3-Chloro-2-hydrazinylpyridine and 2-Chloro-5-nitrobenzoic acid were activated by addition of phosphorus oxychloride and then reduced by Fe to afford **compound 4**. Different carboxylic acid groups were formed into corresponding acyl chloride compounds under dichlorosulfoxide and then reacted with **compound 4** under dichloromethane and DIPEA to afford compounds **TPB1-TPB20**. The structures of the target compounds were proved by ¹H NMR, ¹³C NMR and HRMS (see Supporting information).



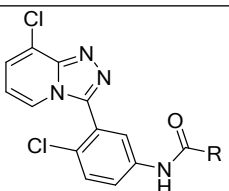
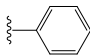
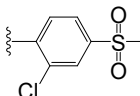
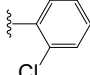
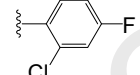
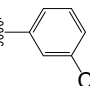
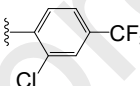
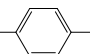
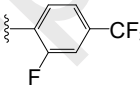
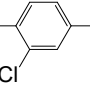
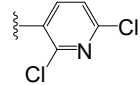
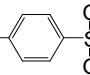
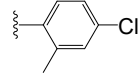
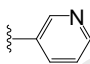
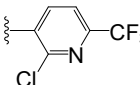
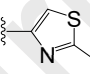
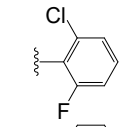
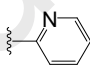
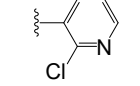
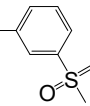
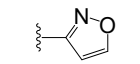
Scheme 1. Synthetic route for compounds **TPB1-TPB20**. Conditions: (a) reflux, 8 h; (b) 80°C, reflux, 4 h; (c) reflux, 3 h; (d) stirred overnight at room temperature.

2.3. Inhibitory activity of compound **TPB1-TPB20** on Hedgehog pathway

To determine whether compounds **TPB1-TPB20** have significant effect on the activation of the Hh pathway, their inhibitory effect was assessed using NIH3T3 cells transfected with 8×Gli-binding site firefly luciferase reporter assay ²⁴. **VIS**, the Smo antagonist, was a control to verify the assay (**Table 1**). The results show that most of our compounds displayed moderate activity against Hh signaling pathway. Among them, compounds **TPB3**, **TPB14**, **TPB15** and **TPB17** offered considerable potency in this assay with IC_{50} of 0.102 μM , 0.096 μM , 0.090 μM and 0.093 μM , respectively (**VIS**, IC_{50} 0.100 μM) (**Table 1**). The result demonstrated that our compounds can block the Hh

signaling pathway at nanomolar concentrations. In contrast, the other compounds showed poor inhibitory activities.

Table 1. Chemical structures and activity of compounds (TPB1-TPB20).

					
Compd	R	IC ₅₀ of Gli-luc reporter (μM)	Compd	R	IC ₅₀ of Gli-luc reporter (μM)
TPB1		0.770 ± 0.070	TPB11		4.274 ± 0.222
TPB2		0.727 ± 0.145	TPB12		8.218 ± 0.457
TPB3		0.102 ± 0.020	TPB13		5.204 ± 0.381
TPB4		2.725 ± 0.334	TPB14		0.096 ± 0.002
TPB5		0.285.5 ± 0.020	TPB15		0.090 ± 0.007
TPB6		1.767 ± 0.307	TPB16		> 10
TPB7		> 10	TPB17		0.093 ± 0.013
TPB8		> 10	TPB18		> 10
TPB9		1.079 ± 0.107	TPB19		> 10
TPB10		2.979 ± 0.299	TPB20		> 10
VIS		0.1000 ± 0.022			

^aIC₅₀ denote the drug concentration that inhibits 50% of Gli-luc reporter. Values represent the mean ± S.D. from 3–5 separate experiments.

2.4. Antiproliferative activities of the compounds against human cancer cell lines

Aberrant activation of the Hh pathway is associated with the development of multiple cancers^{1, 4, 6}. However, clinical application of FDA-approved Smo inhibitors is currently limited to the treatment of adult BCC and AML. To expand the potential use of Smo inhibitors for other cancers, we evaluated the anti-proliferative effects of our novel compounds (**TPB1–TPB20**) by MTT assay against eight human cancer cell lines breast (MDA-MB-231, MDA-MB-468, MCF-7, T47D), glioma (U251), non-small cell lung (A549), and cervical (AN3-CA, Hela). The IC₅₀ values are summarized in **Table 2**. Interestingly, most new compounds had anti-proliferative activity against these cell lines that were significantly better than **VIS**. While **VIS** was somewhat active in MDA-MB-468, AN3-CA and Hela cells with IC₅₀ values of 79.0, 93.0 and 61.7 μ M, respectively, it was >100 μ M for the other five cell lines. This is consistent with previous studies demonstrating that **VIS** had low activity against breast cancer, even though the Hh pathway was active in these cells as evidenced by strong Gli inhibitor activity²⁵. **TPB15** showed the most extensive anti-proliferative activity in 7 of the 8 cell lines tested. Of note, we found that **TPB15** had no effect on growth of MCF-10A cells, a normal breast epithelial cell, whereas **VIS** treatment inhibited their growth. Clonal formation assays were also performed with **TPB15** using the two most sensitive cell lines (MDA-MB-231; MDA-MB-468) (**Fig. S1**). We obtained IC₅₀ values of 5.63 ± 1.51 and 3.28 ± 0.74 μ M, respectively, confirming the anti-growth effect of **TPB15**. To further validate **TPB15**, the EdU assay was performed on MDA-MB-468 and MDA-MB-231 cells. The result showed that the cell-proliferation capacity of these cells treated with **TPB15** was significantly lower compared to the control group (**Fig. S2**).

Table 2. Anti-proliferative effects of compounds (TPB1-TPB20).

Cmpd	IC ₅₀ (μM)								
	MDA-MB-468	MDA-MB-231	MCF-7	T47D	A549	U251	AN3-CA	Hela	MCF10A
TPB1	>100	58.2 ± 2.0	>100	>100	76.9 ± 7.4	73.5 ± 7.1	67.6 ± 7.9	>100	
TPB2	>100	59.9 ± 1.6	92.2 ± 6.9	83.8 ± 2.6	>100	>100	>100	>100	
TPB3	54.8 ± 5.5	66.1 ± 9.1	71.9 ± 16.9	30.2 ± 5.3	52.7 ± 1.7	43.1 ± 9.6	68.4 ± 8.7	>100	
TPB4	>100	>100	58.4 ± 8.1	>100	73.6 ± 7.5	>100	>100	>100	
TPB5	21.6 ± 0.9	>100	78.2 ± 6.0	>100	61.3 ± 12.4	>100	84.8 ± 19.0	>100	
TPB6	>100	>100	94.2 ± 3.9	>100	>100	>100	>100	>100	
TPB7	>100	>100	>100	>100	>100	>100	>100	>100	
TPB8	>100	>100	>100	>100	>100	74.3 ± 1.5	>100	79.8 ± 6.5	
TPB9	>100	92.0 ± 4.4	96.4 ± 11.2	>100	>100	79.0 ± 19.4	>100	75.5 ± 15.5	
TPB10	>100	>100	88.9 ± 10.2	>100	>100	>100	>100	86.4 ± 7.7	
TPB11	>100	37.2 ± 1.3	>100	>100	>100	44.6 ± 5.6	>100	>100	
TPB12	>100	75.0 ± 2.4	>100	>100	>100	>100	>100	>100	
TPB13	>100	>100	81.6 ± 19.7	>100	>100	>100	>100	>100	
TPB14	22.3 ± 1.1	>100	62.8 ± 7.6	70.8 ± 6.8	>100	>100	41.2 ± 12.5	61.9 ± 16.1	
TPB15	28.6 ± 3.2	29.5 ± 3.2	61.5 ± 4.4	42.3 ± 8.2	64.9 ± 37.5	85.2 ± 3.9	44.5 ± 9.8	66.3 ± 14.6	>100
TPB16	34.3 ± 4.8	>100	>100	>100	>100	>100	>100	>100	
TPB17	46.0 ± 7.9	>100	>100	87.6 ± 32.1	46.8 ± 22.3	>100	48.3 ± 7.0	86.3 ± 20.0	
TPB18	57.6 ± 10.1	>100	>100	>100	72.3 ± 2.7	>100	>100	>100	
TPB19	>100	89.7 ± 5.2	>100	>100	35.8 ± 8.1	>100	>100	87.5 ± 25.8	
TPB20	>100	>100	>100	>100	42.7 ± 6.5	>100	>100	>100	
VIS	79 ± 3.2	>100	>100	>100	>100	>100	93 ± 4.5	61.7 ± 7.6	89.5 ± 12.3

^aIC₅₀ denote the drug concentration that inhibits 50% of cell growth. Values represent the mean ± S.D. from 3–5 separate experiments.

2.5. Apoptosis and cycle arrest of cells induced by compound **TPB15**

To understand its mechanism(s) of action, we studied the impact of **TPB15** on cell cycle distribution. In MDA-MB-468 cells (**Fig. 2A, 2C**), **TPB15** arrested cells in G2/M whereas it arrested MDA-MB-231 cells in G0/G1-phase (**Fig. S3A, S3C**) in a dose-dependent manner. In addition, **TPB15** increased apoptosis in the MDA-MB-468 cells (**Fig. 2B, 2D**) and MDA-MB-231 cells (**Fig. S3B, S3D**) in a

concentration-dependent manner. **TPB15** induced 39.70% apoptosis in MDA-MB-468 cells at the highest concentration. To confirm these results, we detected apoptotic proteins by Western blot. With increasing concentrations of **TPB15**, Bcl-2 was reduced while Bax was increased in both cell lines (**Fig. S4**). These results suggest that the increase of apoptosis contributed to the anti-proliferative effect of **TPB15**.

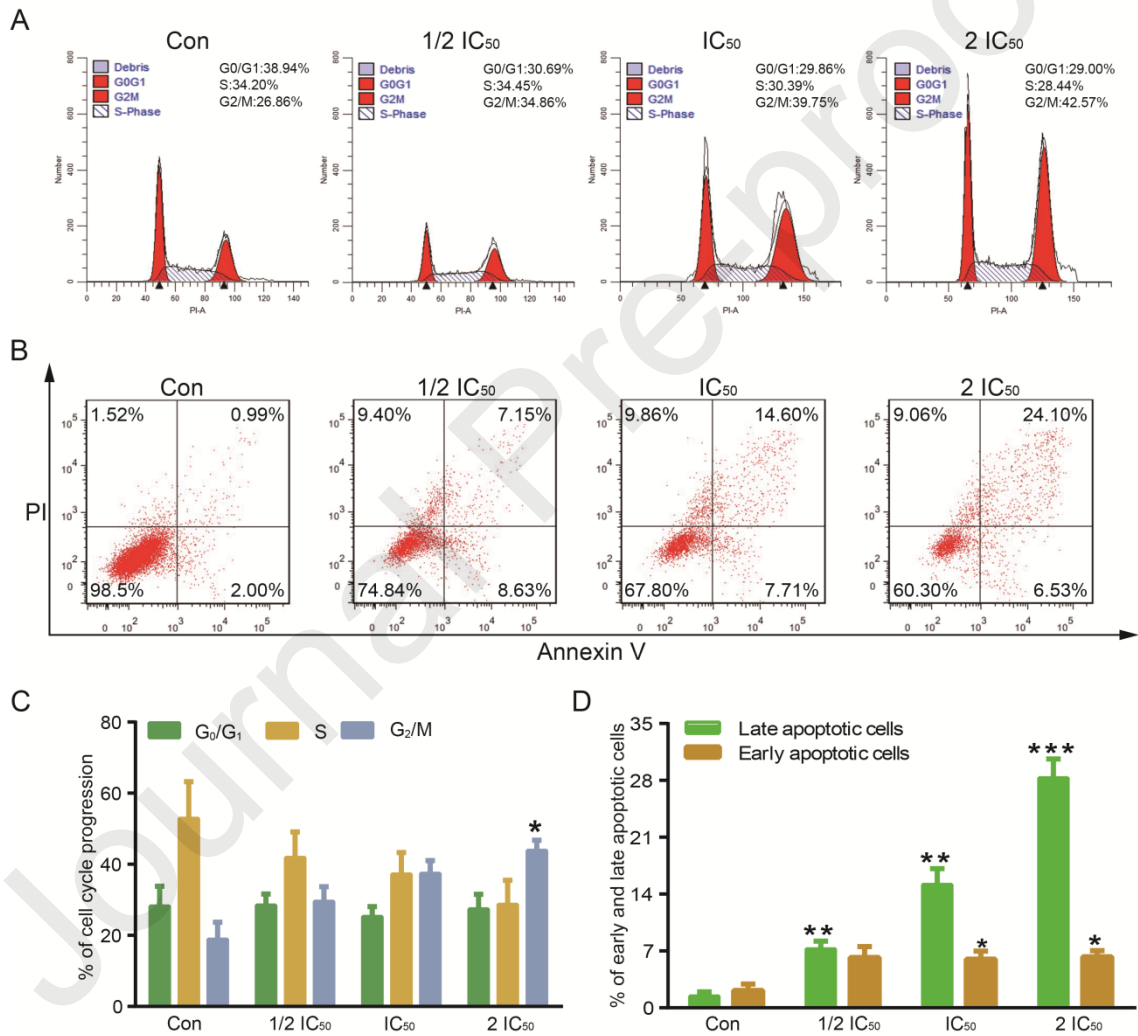


Fig. 2. Analysis of cell cycle and apoptosis in MDA-MB-468 cells. (A) Cells were incubated with **TPB15** (1/2 IC₅₀ = 14 μ M, IC₅₀ = 28 μ M, 2 IC₅₀ = 56 μ M) for 48 h, followed

by fixation, PI staining, and flow cytometric analysis. (B) Cells were treated with **TPB15** for 48 h followed by Annexin V-FITC/PI staining and flow cytometry. Values (C, D) represent the mean \pm S.D. from three independent experiments; (*) $P < 0.05$; (**) $P < 0.01$; (***) $P < 0.001$ vs control (DMSO).

2.6. The binding capacity of the compounds to the Smo protein

Molecular docking, surface plasmon resonance (SPR) and BODIPY-cyclopamine viable cell binding assays were used to evaluate the binding capacity of the compounds to the Smo protein. Considering the flexibility of Smo, the Induce-fit docking (IFD) method was used to elucidate the binding model of potent compounds. IFD allows the movement of both side chains from binding site residues and the rotatable bonds from ligand during the docking process ²⁶. The complex structure of **VIS** was retrieved from the RCSB database (PDB entry: 5L7I ²⁷). The key residues Asp384, Arg400, Gln477, Phe484, Tyr394 were selected for the grid box of the binding site ²⁸.

The docking results demonstrated that the binding modes of compound **TPB14**, **TPB15**, **TPB17**, and **TPB3** were similar to that of **VIS**. As we expected, they occupied binding sites comprised by the entrance of the membrane and the transmembrane domain, especially TM5, TM6 and TM7 (**Fig. 3A**). Dichloropyridinyl group of **TPB15** oriented towards the extracellular domain and the entrance of TMD pocket. The N-4-[1,2,4]triazolo[4,3-a] pyridinyl group, instead of pyridine group from **VIS**, was deeply buried in the core of transmembrane helixes (TM5, TM6 and TM7). The arrangement was stabilized by H-bonds and the pi-pi interaction mentioned below. The core structure amide linker formed two H-bonds: NH from amide linker and the C=O from the main chain of Asp384; C=O from amide and the NH from the side chain of

Glu518 (**Fig. 3A**). Furthermore, the N-4-[1,2,4]triazolo[4,3-a] pyridinyl group could be fixed by cation-pi interactions with Arg400 and by pi-pi interactions with Trp281, stabilizing the binding conformation. The N atoms from triazolo ring and the OH from side chain of Tyr394 also formed H-bonds, which also benefited the conformation. Compounds **TPB8** and **TPB20** have more flexibility because of the smaller five-membered ring, which led to weaker binding results and anti-proliferative activities. Compared with **TPB15**, compound **TPB5** had subtle structural differences. When dichloropyridinyl replaced by dichlorophenyl, the electron-deficiency of the Ar ring led to a little weaker binding. The same phenomena were also evident between compounds **TPB17** and **TPB13**. It was worth noting that the difference of 2-position substitute of phenyl in compounds **TPB13** and **TPB14**: F atom for compound **TPB13** and Cl atom for **TPB14**. It is possible that the conjugation effect from Cl atom decreased the pi-pi interaction with Phe484. As the typical electron-withdrawing groups, the methylsulfone moiety from **TPB10** had the steric hindrance at meta-position of phenyl comparing to Cl from **TPB3**. This might explain why **TPB10** had low activity (2.979 μM) while **TPB3** showed potent activity (0.102 μM). The structure-activity relationship is summarized in **Fig. 3B**.

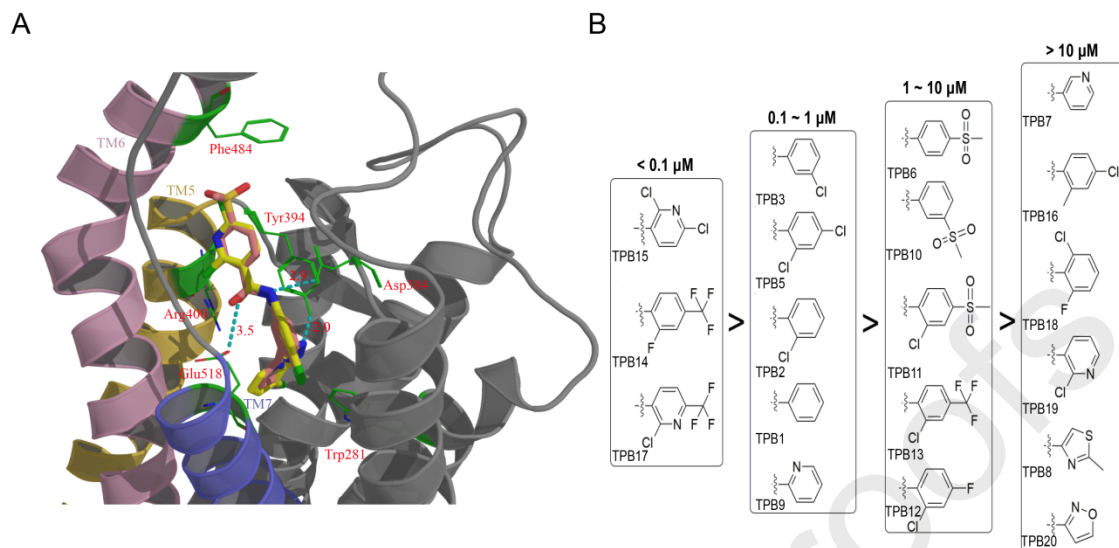


Fig. 3. The binding conformation of **TPB15** compared to **VIS**. (A) IFD of **TPB15** (yellow) and **VIS** (pink). (B) Structure-activity relationships of our novel compounds. Blue dot line represents the H-bonds, and the number on it is the distance of the H-bone.

Since compounds **TPB3**, **TPB14**, **TPB15** and **TPB17** showed improved potency, SPR experiments were used to characterize the interaction of these compounds with Smo protein compared to **VIS**. The results showed that the equilibrium dissociation constants (KD) between compounds **TPB3**, **TPB14** and Smo were 1.21×10^{-5} M and 1.36×10^{-5} M, respectively, while **VIS** was 9.75×10^{-8} M (Table 3, Fig. S5). Surprisingly, compounds **TPB15** and **TPB17** exhibited the most powerful interactions with Smo (KD values, 1.03×10^{-8} M and 1.06×10^{-8} M). These data indicated that **TPB15** and **TPB17** bind significantly tighter with Smo protein than **VIS**.

Table 3. The binding strength of **TPB3**, **TPB14**, **TPB15**, **TPB17** and **VIS** to the Smo receptor

Cmpd	ka^a (1/Ms)	kd^b (1/s)	Rmax^c (RU)	KA^d (1/M)	KD^e (M)
TPB3	101	1.23×10^{-3}	41.2	8.21×10^4	1.21×10^{-5}
TPB14	111	1.51×10^{-3}	49.2	7.35×10^4	1.36×10^{-5}
TPB15	360	3.75×10^{-6}	90.5	9.71×10^7	1.03×10^{-8}
TPB17	260	2.75×10^{-6}	8.44	9.43×10^7	1.06×10^{-8}
VIS	179	1.74×10^{-5}	4.63	1.03×10^7	9.75×10^{-8}

^a ka = association rate constant

^b kd = dissociation rate constant

^c Rmax = maximum resonance response at equilibrium

^d KA = the equilibrium association constant

^e KD = the equilibrium dissociation constant

BODIPY-cyclopamine viable cell binding assay was used to determine whether our compounds can bind directly to the Smo protein ²⁹. Green-fluorescence was observed in cells after incubation with BODIPY-cyclopamine (**Fig. 4B**). Incubation with unlabeled cyclopamine resulted in decreased green fluorescence, indicating that unlabeled cyclopamine competitively inhibits the binding of BODIPY-cyclopamine. Cells treated with **TPB15** displayed a clear dose-dependent reduction in the green fluorescence indicating that compound **TPB15** binds to Smo protein intracellularly.

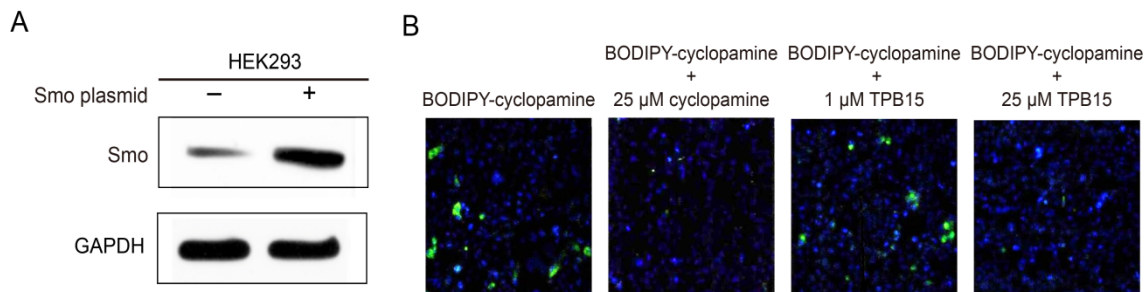


Fig. 4. (A) Western blot analysis of the Smo protein in the HEK293 cells transfected with WT-Smo plasmid. (B) BODIPY-cyclopamine viable cell binding assay.

2.7. Compounds inhibited the expression of Hedgehog pathway signaling proteins and mRNA

To verify the mechanism of action, the time- and dose-dependent effects of **TPB3**, **TPB14**, **TPB15** and **TPB17** on Smo protein and mRNA expression were characterized by Western blot and qRT-PCR. The expression of Smo protein and mRNA was markedly suppressed in a dose- and time-dependent manner (**Fig. 5**). We also evaluated the effect of **TPB15** on other members of the Hedgehog pathway. As observed with Smo, the expression of Shh, Gli1 and Ptch2 protein and mRNA was significantly suppressed in a dose- and time-dependent manner (**Fig. S6**). Therefore, these data further support that compound **TPB15** effectively inhibits the Hh signaling pathway.

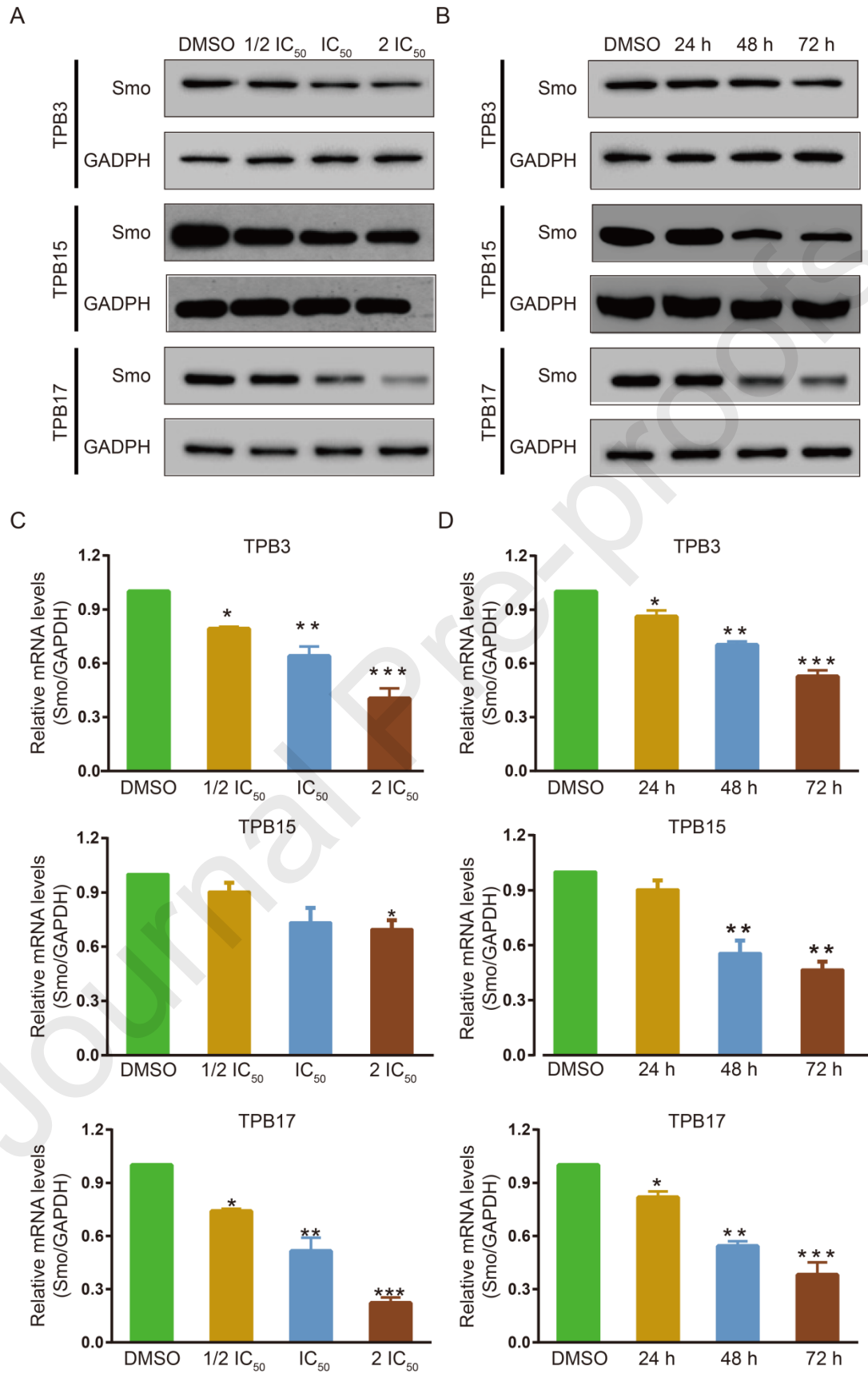


Fig. 5. Effect of Smo inhibitors on Smo protein and mRNA in MDA-MB-468 cells. Cells treated with **TPB3** (55 μ M), **TPB15** (28 μ M) or **TPB17** (50 μ M) for 48 h were harvested and processed for western blot analysis (A) and qRT-PCR (C). Cells treated with compounds for 24-72 h were processed by western blot analysis (B) and qRT-PCR (D). GAPDH was used as an internal control. Data represent the mean \pm S.D. from 3 experiments. (*) $P < 0.05$; (**) $P < 0.01$; (***) $P < 0.001$ vs control (DMSO).

2.8. Smo localization upon treatment with **TPB15**

Smo acts on the primary cilium, transmitting Hh signals, while Smo localization to cilia is a key regulatory step in Hh pathway activation³⁰. We tested whether our compounds can inhibit Hh pathway activation through disruption of Smo translocation. Primary cilia were visualized by immunofluorescence labeled with anti-acetylated α -tubulin antibodies. NIH3T3 cells were treated with **TPB15** or **VIS** for 24 h, in the presence or absence of 200 nM Smo agonist SAG. Confocal imaging revealed that **TPB15** inhibited SAG-induced Smo localization to the primary cilia similar to **VIS** (**Fig. 6A**). In addition, Smo protein levels were significantly reduced in the cilia of MDA-MB-468 cells following **TPB15** or **VIS** treatment (**Fig. 6B**). Blocking the translocation of Smo to the primary cilia has been shown to reduce Gli1 expression and its target genes associated with proliferation, survival and metastasis³¹. These results indicate that Hh signaling can be suppressed by **TPB15** through blocking Smo translocation into the primary cilia.

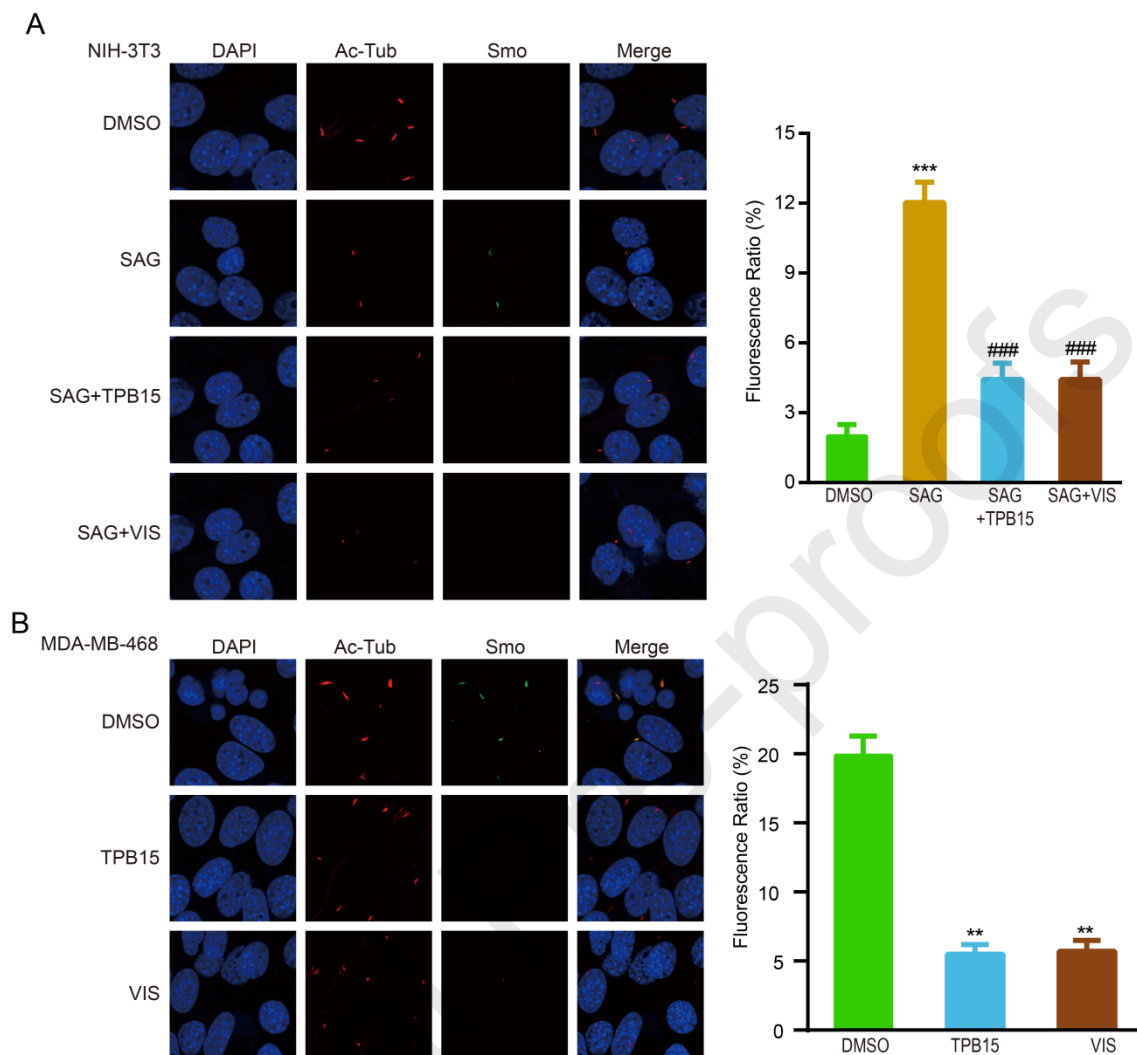


Fig. 6. Effect of **TPB15** on Smo localization. Confocal imaging of primary cilia of NIH3T3 cells (A) and MDA-MB-468 cells (B) treated with **VIS** or **TPB15** (28 μ M) for 24 h in the presence or absence of SAG after immunostaining with anti-acetylated α -tubulin and Smo antibodies. ***, $P < 0.001$, **, $P < 0.01$ vs DMSO; ###, $P < 0.001$ vs SAG.

2.9. Acute toxicity test

The new compounds showed broad anti-proliferative activity against cancer cell lines *in vitro* with low toxicity against normal breast epithelial MCF-10A cells. We

hypothesized that our compounds have low toxicity *in vivo*. To verify this hypothesis, two of our most active compounds were selected for an acute *in vivo* toxicity test. The LD₅₀ of **TPB3**, **TPB15** and **VIS** were determined using Kunming mice by intragastric administration according to the improved Karber's method ³². **TPB3** (LD₅₀ > 5000 mg/kg) and **TPB15** (LD₅₀ = 3875 mg/kg) had higher LD₅₀ and thus lower toxicity compared to **VIS** (LD₅₀ = 2008 mg/kg) (Table 4).

Table 4. Acute toxicity of **TPB3**, **TPB15** and **VIS**

Cmpd	Dose (mg/kg)	Mortality (D/T)		Mortality (%)	LD ₅₀ (mg/kg)
		Female	Male		
TPB3	5000	0/5	0/5	0	> 5000
	3008	1/5	0/5	10	
	3453	2/5	1/5	30	
TPB15	3965	3/5	2/5	50	3875
	4552	3/5	3/5	60	
	5226	4/5	3/5	70	
VIS	741	1/5	0/5	10	2008
	1111	1/5	2/5	30	
	1778	3/5	2/5	50	
	2667	4/5	2/5	60	
	4000	4/5	4/5	80	

D/T: dead/treated mice. 95% confidence intervals of **TPB15** were between 2807 and 4956 mg/kg. 95% confidence intervals of **VIS** were between 788 and 3623 mg/kg.

2.10. **TPB15** inhibits xenograft tumor growth *in vivo*

To evaluate the anti-tumor effect of compound **TPB15** *in vivo*, a subcutaneous MDA-MB-468 xenograft model was used. Tumor volume was recorded every other day and the body weight was recorded every day. **TPB15** and **VIS** were dosed at 80 mg/kg

and 100 mg/kg per day, respectively (intragastric administration). Smo inhibitors did not affect mouse body weight (**Fig. 7A**). The reduction in tumor volume of **VIS**-treated group (100 mg/kg) reached 55.78% compared to the vehicle control, while **TPB15** (80 mg/kg) reduced the tumor volume by 64.97% (**Fig. 7B**). Thus, **TPB15** has significant inhibitory effects on tumor growth in vivo without evidence of toxicity.

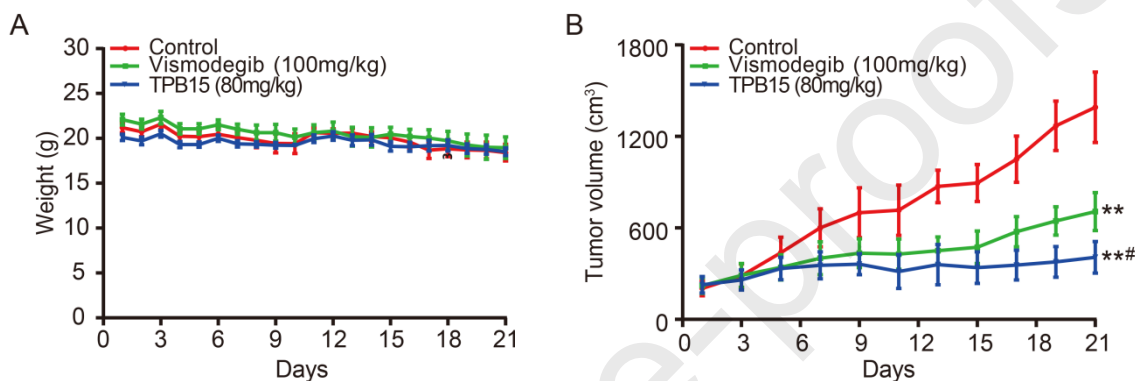


Fig. 7. Effect of **TPB15** on growth of a breast cancer xenograft. Body weight (A) and tumor volume (B) were expressed as mean \pm SD (n=5/group). **, p<0.01 compared to control; #, p<0.05 compared to Vismodegib group.

3. Discussion

In summary, we have developed a series of novel [1,2,4]triazolo[4,3-a]pyridines as potent Smo inhibitors that exhibited anti-proliferative activity against a variety of cancer cell lines, especially TNBC. The compounds **TPB14**, **TPB15** and **TPB17** demonstrated nanomolar inhibition of the Gli-luciferase reporter assay indicating that the design of 8-chloro-[1,2,4]triazolo[4,3-a]pyridines was successful. Molecular docking simulations indicated that our compounds have a similar binding mode as **VIS** to Smo protein. Surprisingly, the SPR assay demonstrated that compounds **TPB15** and **TPB17** interacted

with Smo protein with stronger affinity than **VIS**. The potency may be related to the novel scaffold that potentially increases the H-bond interactions with the hinge region of Smo. Compounds containing a 3-chlorophenyl and 2,6-dichloro-3-pyridyl moiety, **TPB15** and **TPB3**, respectively, showed extensive anti-proliferative activity in various cell lines. This indicated that the introduction of chlorine atoms in phenyl or pyridyl moieties might improve biological activity. Global cancer epidemic statistics shown that breast cancer accounts for 11.6% of all the cancer incidence, the second leading cause of cancer death among women after lung cancer, and TNBC accounts for about 15~20% of breast cancers³³. Currently, there is no FDA-approved targeted therapy for TNBC, so patients have to undergo a systemic treatment strategy based on conventional chemotherapy and radiotherapy³⁴. Evidence suggests that about 30% of the TNBCs have paracrine activation in the Hh signaling pathway; SMO inhibitors could represent therapeutics of interest for a significant number of women who diagnosed with TNBC²⁰. Our results provide evidence that four of the novel compounds suppress the growth of human breast cancer cells in vitro. **TPB15** induced cell apoptosis and cycle arrest in breast cancer cells, and reduced expression of Bcl-2 while increased the Bax. Mechanisms results showed that **TPB15** effectively suppressed protein and mRNA expression of members of the Hh pathway, which downregulated Hh target gene expression. Imaging studies demonstrated that **TPB15** suppressed Hh signaling through blocking Smo translocation into the cilia. Consistent with our in vitro data, we also found **TPB15** significantly reduced the tumor volume with low toxicity. Taken together, our results show that the [1,2,4]triazolo[4,3-a]pyridine scaffold represents a novel platform for the development of a novel class of Hh pathway inhibitors for the treatment of TNBC.

4. Experimental section

4.1. General

Unless otherwise specified, all chemical and biological reagents are purchased from commercial suppliers and used without further decontamination. All reactions were monitored using thin-layer chromatography (TLC) on silica gel plates at 254 nm under a UV light. ^1H and ^{13}C NMR spectra were recorded on a BRUKER AVIII 400 MHz and 101 MHz spectrometers. High resolution mass spectra (HR-ESI-MS) were determined on Orbitrap Fusion Tribrid (Q-OT-qIT) mass spectrometer (Thermo Fisher Scientific, Bremen, German). The purity of the targeted compound was measured by high performance liquid chromatography (HPLC), performed on the LC-2010CHT (Shimadzu, Japan) using Waters XTERRA MS C18 column ($3.5\ \mu\text{m}$ $2.1\times 100\text{mm}$, Waters , USA) , eluting with a mixture of solvents MeOH (A) and 0.1% formic acid aqueous (B) from VA:VB = 20:80 to 80:20. Peaks were detected at 254 nm with a flow rate of 0.25 mL/min.

4.2. Synthesis

4.2.1 Synthesis of 4-chloro-3-(8-chloro-[1,2,4]triazolo[4,3-a]pyridin-3-yl)aniline (Compound 4)

As shown in the **Scheme 1.**, phosphorus oxychloride (400 ml) was added dropwise at room temperature to a mixture of 3-Chloro-2-hydrazinylpyridine (**Compound 1**, 20.0 g, 0.139 mol) and 2-Chloro-5-nitrobenzoic acid (**Compound 2**, 30.0 g, 0.149 mol). The mixture was then vigorously stirred at reflux temperature for 8 h. After cooling to room temperature, the reaction solution was poured into ice water and filtered to give the 8-chloro-3-(2-chloro-5-nitrophenyl)-[1,2,4]triazolo[4,3-a]pyridine (**Compound 3**, 37.8 g,

yield: 88%) as a gray solid. $^1\text{H-NMR}$ (400 MHz, $\text{d}_6\text{-DMSO}$) δ = 8.64 (s, 1H), 8.53 (d, J = 7.5 Hz, 1H), 8.29 (d, J = 6.6 Hz, 1H), 8.09 (d, J = 8.9 Hz, 1H), 7.74 (d, J = 7.0 Hz, 1H), 7.08 (t, J = 6.9 Hz, 1H). ESI-MS for $\text{C}_{12}\text{H}_6\text{Cl}_2\text{N}_4\text{O}_2$ ($[\text{M}+\text{H}]^+$) Calcd: 308.99; Found: 309.10. To a suspension of **Compound 3** (44.0 g, 0.142 mol) in 250 ml saturated aq. NH_4Cl and 250 mL of EtOH was added Fe powder (31.8 g, 0.569 mol). The reaction mixture was stirred at 80°C for 4 hours, cooled down to room temperature and then filtered through Celite. The filter cake was washed with EtOH. The solution was concentrated in vacuo, and the residue was dissolved in DCM, then washed with saturated NaHCO_3 . The organic phase was dried over anhydrous Na_2SO_4 , filtered and concentrated in vacuo. The residue was purified by silica gel column (DCM/MeOH=20/1) to afford 4-chloro-3-(8-chloro-[1,2,4]triazolo[4,3-a]pyridin-3-yl)aniline (**Compound 4**, 14.2 g, yield: 35.9%) as a white solid. $^1\text{H-NMR}$ (400 MHz, $\text{d}_6\text{-DMSO}$) δ = 8.03 (d, J = 6.9 Hz, 1H), 7.67 (d, J = 7.1 Hz, 1H), 7.33 (d, J = 8.7 Hz, 1H), 7.02 (t, J = 7.1 Hz, 1H), 6.86 – 6.81 (m, 1H), 5.65 (s, 1H), ESI-MS for $\text{C}_{12}\text{H}_8\text{Cl}_2\text{N}_4$ ($[\text{M}+\text{H}]^+$) Calcd: 279.01; Found: 279.10.

4.2.2 synthesis of *N*-(4-chloro-3-(8-chloro-[1,2,4]triazolo[4,3a]pyridin-3-yl)phenyl)benzamide (**TPB1**)

Thionyl chloride (0.356 g; 3 mmol) was added to a mixture of benzoic acid (0.122 g, 1 mmol) in toluene and the mixture was heated at reflux for 3 hours. The reaction was cooled to room temperature and the solvent was removed under reduced pressure. The resultant acid chloride was dropwised to a mixture of **Compound 4** (0.279 g, 1 mmol) and DIPEA (0.258g, 2 mmol) in dichloromethane (15ml) at room temperature. The

solution was stirred for overnight, then concentrated in vacuo. The residue was purified by silica gel column (DCM/MeOH=20/1) to afford compound **TPB1** (0.382 g, yield: 75%) as a white solid. purity: 99%; mp: 242.3-244.1°C; ¹H-NMR (d6-DMSO): δ = 10.65 (s, 1H), 8.21 (d, J = 2.5 Hz, 1H), 8.17 (dd, J = 7.0, 0.8 Hz, 1H), 8.13 (dd, J = 8.9, 2.7 Hz, 1H), 8.02 – 7.94 (m, 2H), 7.76 (dd, J = 8.9, 1.6 Hz, 1H), 7.70 (dt, J = 7.2, 0.9 Hz, 1H), 7.65 – 7.59 (m, 1H), 7.55 (td, J = 7.1, 1.3 Hz, 2H), 7.06 (t, J = 7.1 Hz, 1H); ¹³C-NMR (d6-DMSO): δ = 166.36 (s), 147.97 (s), 146.19 (s), 139.24 (s), 134.84 (s), 132.41 (s), 130.91 (s), 128.97 (s), 128.21 (s), 127.92 (s), 127.55 (s), 125.60 (s), 124.52 (s), 124.40 (s), 124.13 (s), 120.65 (s), 114.88 (s); HR-ESI-MS for C₁₉H₁₃ON₄Cl₂ ([M+H]⁺) Calcd: 383.0461; Found: 383.0460.

4.2.3 *Synthesis of 2-chloro-N-(4-chloro-3-(8-chloro-[1,2,4]triazolo[4,3-a]pyridin-3-yl)phenyl)-benzamide (TPB2)*

Thionyl chloride (0.356 g; 3 mmol) was added to a mixture of 2-chlorobenzoic acid (0.156 g, 1 mmol) in toluene and the mixture was heated at reflux for 3 hours. The reaction was cooled to room temperature and the solvent was removed under reduced pressure. The resultant acid chloride was dropwised to a mixture of **Compound 4** (0.279 g, 1 mmol) and DIPEA (0.258g, 2 mmol) in dichloromethane (15ml) at room temperature. The solution was stirred for overnight, then concentrated in vacuo. The residue was purified by silica gel column (DCM/MeOH=20/1) to afford **TPB2** (0.281 g, yield: 68%); purity: 98%; mp: 247.3-248.5°C; ¹H-NMR (d6-DMSO): δ = 10.95 (s, 1H), 8.24 – 8.07 (m, 2H), 8.01 (dd, J = 8.9, 2.6 Hz, 1H), 7.74 (dd, J = 25.8, 8.0 Hz, 2H), 7.67 – 7.57 (m, 2H), 7.56 – 7.40 (m, 2H), 7.06 (t, J = 7.1 Hz, 1H); ¹³C-NMR (d6-DMSO): δ =

165.78 (s), 148.00 (s), 146.17 (s), 138.87 (s), 136.87 (s), 131.92 (s), 131.11 (s), 130.38 (s), 130.23 (s), 129.45 (s), 127.94 (s), 127.84 (s), 125.87 (s), 124.19 (s), 123.87 (s), 123.76 (s), 120.63 (s), 114.87 (s), 99.98 (s); HR-ESI-MS for $C_{19}H_{10}ON_4Cl_3$ ($[M-H]^+$) Calcd: 414.9920; Found: 414.9929.

4.2.4 synthesis of 3-chloro-N-(4-chloro-3-(8-chloro-[1,2,4]triazolo[4,3-a]pyridin-3-yl)phenyl)benzamide (**TPB3**)

Thionyl chloride (0.356 g; 3 mmol) was added to a mixture of 3-chlorobenzoic acid (0.156 g, 1 mmol) in toluene and the mixture was heated at reflux for 3 hours. The reaction was cooled to room temperature and the solvent was removed under reduced pressure. The resultant acid chloride was dropwised to a mixture of **Compound 4** (0.279 g, 1 mmol) and DIPEA (0.258g, 2 mmol) in dichloromethane (15ml) at room temperature. The solution was stirred for overnight, then concentrated in vacuo. The residue was purified by silica gel column (DCM/MeOH=20/1) to afford **TPB3** (0.342 g, yield: 83%); purity: 98%; mp: 282.1-283.1°C; 1H -NMR (d6-DMSO): δ = 10.73 (s, 1H), 8.21 – 8.14 (m, 2H), 8.11 (dd, J = 8.9, 2.6 Hz, 1H), 8.04 (t, J = 1.9 Hz, 1H), 7.94 (dt, J = 7.9, 1.3 Hz, 1H), 7.78 (d, J = 8.9 Hz, 1H), 7.74 – 7.67 (m, 2H), 7.60 (t, J = 7.9 Hz, 1H), 7.06 (t, J = 7.1 Hz, 1H); ^{13}C -NMR (d6-DMSO): δ = ^{13}C NMR (101 MHz, DMSO) δ 164.86 (s), 147.99 (s), 146.14 (s), 140.14 (s), 138.93 (s), 136.78 (s), 133.76 (s), 132.24 (s), 131.02 (s), 130.98 (s), 127.93 (s), 127.86 (s), 127.07 (s), 125.66 (s), 124.65 (s), 124.49 (s), 124.15 (s), 120.65 (s), 114.90 (s); HR-ESI-MS for $C_{19}H_{10}ON_4Cl_3$ ($[M-H]^+$) Calcd: 414.9920; Found: 414.9931.

4.2.5 Synthesis of 4-chloro-N-(4-chloro-3-(8-chloro-[1,2,4]triazolo[4,3-a]pyridin-3-yl)phenyl)benzamide (**TPB4**)

Thionyl chloride (0.356 g; 3 mmol) was added to a mixture of 2-chlorobenzoic acid (0.156 g, 1 mmol) in toluene and the mixture was heated at reflux for 3 hours. The reaction was cooled to room temperature and the solvent was removed under reduced pressure. The resultant acid chloride was dropwised to a mixture of **Compound 4** (0.279 g, 1 mmol) and DIPEA (0.258g, 2 mmol) in dichloromethane (15ml) at room temperature. The solution was stirred for overnight, then concentrated in vacuo. The residue was purified by silica gel column (DCM/MeOH=20/1) to afford **TPB4** (0.301 g, yield: 73%); purity: 99%; mp: >290°C; ¹H-NMR (d6-DMSO): δ = 10.70 (s, 1H), 8.20 – 8.14 (m, 2H), 8.11 (dd, J = 8.9, 2.6 Hz, 1H), 8.04 – 7.97 (m, 2H), 7.77 (d, J = 8.8 Hz, 1H), 7.71 (dd, J = 7.2, 0.8 Hz, 1H), 7.68 – 7.60 (m, 2H), 7.06 (t, J = 7.1 Hz, 1H); ¹³C-NMR (d6-DMSO): δ = 166.36 (s), 147.97 (s), 146.19 (s), 139.24 (s), 134.84 (s), 132.41 (s), 130.91 (s), 128.97 (s), 128.21 (s), 127.92 (s), 127.55 (s), 125.60 (s), 124.52 (s), 124.40 (s), 124.13 (s), 120.65 (s), 114.88 (s); HR-ESI-MS for C₁₉H₁₀ON₄Cl₃ ([M-H]⁺) Calcd: 414.9920; Found: 414.9930.

4.2.6 Synthesis of 2,4-dichloro-N-(4-chloro-3-(8-chloro-[1,2,4]triazolo[4,3-a]pyridine-3-yl)phenyl)benzamide (**TPB5**)

Thionyl chloride (0.356 g; 3 mmol) was added to a mixture of 2,4-dichlorobenzoic acid (0.191 g, 1 mmol) in toluene and the mixture was heated at reflux for 3 hours. The reaction was cooled to room temperature and the solvent was removed under reduced pressure. The resultant acid chloride was dropwised to a mixture of **Compound 4** (0.279 g, 1 mmol) and DIPEA (0.258g, 2 mmol) in dichloromethane (15ml) at room temperature. The solution was stirred for overnight, then concentrated in vacuo. The residue was purified by silica gel column (DCM/MeOH=20/1) to afford **TPB5** (0.281 g, yield: 63%);

purity: 98%; mp: 212.3-213.9°C; ¹H-NMR (d6-DMSO): δ = 10.98 (s, 1H), 8.16 (d, J = 6.9 Hz, 1H), 8.11 (d, J = 2.6 Hz, 1H), 8.05 – 7.95 (m, 1H), 7.80 (d, J = 2.0 Hz, 1H), 7.77 (d, J = 8.8 Hz, 1H), 7.70 (dd, J = 7.7, 5.9 Hz, 2H), 7.64 – 7.56 (m, 1H), 7.06 (t, J = 7.1 Hz, 1H); ¹³C-NMR (d6-DMSO): δ = 164.86 (s), 148.00 (s), 146.13 (s), 138.68 (s), 135.69 (s), 135.65 (s), 131.71 (s), 131.15 (s), 130.87 (s), 129.80 (s), 128.05 (s), 127.99 (s), 127.95 (s), 125.91 (s), 124.19 (s), 123.93 (s), 123.80 (s), 120.63 (s), 114.87 (s); HR-ESI-MS for C₁₉H₉ON₄Cl₄ ([M-H]⁺) Calcd: 448.9530; Found: 448.9547.

4.2.7 Synthesis of *N*-(4-chloro-3-(8-chloro-[1,2,4]triazolo[4,3-*a*]pyridin-3-yl)phenyl)-4-(methylsulfonyl)benzamide (**TPB6**)

Thionyl chloride (0.356 g; 3 mmol) was added to a mixture of 4-(methylsulfonyl)benzoic acid (0.200 g, 1 mmol) in toluene and the mixture was heated at reflux for 3 hours. The resultant acid chloride was dropwised to a mixture of **Compound 4** (0.279 g, 1 mmol) and DIPEA (0.258g, 2 mmol) in dichloromethane (15ml) at room temperature. The solution was stirred for overnight, then concentrated in vacuo. The residue was purified by silica gel column (DCM/MeOH=20/1) to afford **TPB6** (0.409 g, yield: 89%); purity: 97%; mp: 267.6-268.9°C; ¹H-NMR (d6-DMSO): δ = 10.88 (s, 1H), 8.20 (dd, J = 8.7, 2.1 Hz, 3H), 8.17 (dd, J = 6.9, 0.8 Hz, 1H), 8.12 (dd, J = 8.7, 2.7 Hz, 3H), 7.79 (d, J = 8.8 Hz, 1H), 7.71 (dd, J = 7.2, 0.8 Hz, 1H), 7.06 (t, J = 7.1 Hz, 1H), 3.31 (s, 3H); ¹³C-NMR (d6-DMSO): δ = 165.13 (s), 148.00 (s), 146.12 (s), 143.92 (s), 139.32 (s), 138.84 (s), 131.03 (s), 129.24 (s), 128.03 (s), 127.95 (s), 127.67 (s), 125.72 (s), 124.69 (s), 124.53 (s), 124.15 (s), 120.65 (s), 114.90 (s); HR-ESI-MS for C₂₀H₁₅O₃N₄Cl₂S ([M+H]⁺) Calcd: 461.0242; Found: 461.0234.

4.2.8 Synthesis of *N*-(4-chloro-3-(8-chloro-[1,2,4]triazolo[4,3-*a*]pyridin-3-yl)phenyl)

nicotinamide (TPB7)

Thionyl chloride (0.356 g; 3 mmol) was added to a mixture of nicotinic acid (0.123 g, 1 mmol) in toluene and the mixture was heated at reflux for 3 hours. The reaction was cooled to room temperature and the solvent was removed under reduced pressure. The resultant acid chloride was dropwised to a mixture of **Compound 4** (0.279 g, 1 mmol) and DIPEA (0.258g, 2 mmol) in dichloromethane (15ml) at room temperature. The solution was stirred for overnight, then concentrated in vacuo. The residue was purified by silica gel column (DCM/MeOH=20/1) to afford **TPB7** (0.308 g, yield: 81%); purity: 98%; mp: 276.7-277.2°C; ¹H-NMR (d6-DMSO): δ = 10.81 (s, 1H), 9.10 (dd, J = 2.4, 1.0 Hz, 1H), 8.75 (dd, J = 4.8, 1.7 Hz, 1H), 8.29 (dt, J = 8.1, 2.0 Hz, 1H), 8.17 – 8.10 (m, 2H), 8.08 (dd, J = 8.9, 2.6 Hz, 1H), 7.74 (d, J = 8.9 Hz, 1H), 7.67 (dd, J = 7.2, 0.8 Hz, 1H), 7.55 (ddd, J = 8.0, 4.8, 0.9 Hz, 1H), 7.02 (t, J = 7.1 Hz, 1H); ¹³C-NMR (d6-DMSO): δ = 164.85 (s), 152.84 (s), 149.16 (s), 147.94 (s), 146.07 (s), 138.86 (s), 135.98 (s), 130.96 (s), 130.51 (s), 127.88 (s), 127.87 (s), 125.65 (s), 124.55 (s), 124.42 (s), 124.07 (s), 124.00 (s), 120.62 (s), 114.85 (s); HR-ESI-MS for C₁₈H₁₀ON₃Cl₂ ([M-H]⁺) Calcd: 382.0262; Found: 382.0273.

4.2.9 Synthesis of *N*-(4-chloro-3-(8-chloro-[1,2,4]triazolo[4,3-*a*]pyridin-3-yl)phenyl)-2-methylthiazole-4-carboxamide (**TPB8**)

-2-methylthiazole-4-carboxamide (TPB8)

Thionyl chloride (0.356 g; 3 mmol) was added to a mixture of 3-(methylsulfonyl)benzoic acid (0.156 g, 1 mmol) in toluene and the mixture was heated at reflux for 3 hours. The reaction was cooled to room temperature and the solvent was removed under reduced pressure. The resultant acid chloride was dropwised to a mixture of **Compound 4** (0.279 g, 1 mmol) and DIPEA (0.258g, 2 mmol) in dichloromethane

(15ml) at room temperature. The solution was stirred for overnight, then concentrated in vacuo. The residue was purified by silica gel column (DCM/MeOH=20/1) to afford **TPB8** (0.278 g, yield: 69%); purity: 98%; mp: 238.6-239.7°C; ¹H-NMR (d6-DMSO): δ = 10.62 (s, 1H), 8.30 (s, 1H), 8.25 (d, J = 2.7 Hz, 1H), 8.21 – 8.06 (m, 2H), 7.68 (dd, J = 15.3, 8.0 Hz, 2H), 7.01 (t, J = 7.1 Hz, 1H), 2.73 (s, 3H); ¹³C-NMR (d6-DMSO): δ = 166.97 (s), 159.87 (s), 149.30 (s), 147.89 (s), 146.04 (s), 138.63 (s), 130.81 (s), 127.87 (s), 127.74 (s), 126.30 (s), 125.42 (s), 124.59 (s), 124.07 (s), 120.59 (s), 114.84 (s), 104.23 (s), 19.26 (s); HR-ESI-MS for C₁₇H₁₂ON₅Cl₂S ([M+H]⁺) Calcd: 404.0140; Found: 404.0130.

4.2.10 Synthesis of N-(4-chloro-3-(8-chloro-[1,2,4]triazolo[4,3-a]pyridin-3-yl)phenyl)picolinamide (TPB9)

Thionyl chloride (0.356 g; 3 mmol) was added to a mixture of picolinic acid (0.123 g, 1 mmol) in toluene and the mixture was heated at reflux for 3 hours. The reaction was cooled to room temperature and the solvent was removed under reduced pressure. The resultant acid chloride was dropwised to a mixture of **Compound 4** (0.279 g, 1 mmol) and DIPEA (0.258g, 2 mmol) in dichloromethane (15ml) at room temperature. The solution was stirred for overnight, then concentrated in vacuo. The residue was purified by silica gel column (DCM/MeOH=20/1) to afford **TPB9** (0.202 g, yield: 53%); purity: 97%; mp: 224.6-225.8°C; ¹H-NMR (d6-DMSO): δ = 11.05 (s, 1H), 8.72 (ddd, J = 4.8, 1.7, 0.9 Hz, 1H), 8.33 (d, J = 2.6 Hz, 1H), 8.21 (dd, J = 8.9, 2.6 Hz, 1H), 8.16 – 8.08 (m, 2H), 8.04 (td, J = 7.7, 1.7 Hz, 1H), 7.73 (d, J = 8.9 Hz, 1H), 7.66 (ddd, J = 6.2, 3.3, 1.8 Hz, 2H), 7.02 (t, J = 7.0 Hz, 1H); ¹³C-NMR (d6-DMSO): δ = 163.49 (s), 149.90 (s), 148.94 (s), 147.90 (s), 146.03 (s), 138.63 (s), 138.48 (s), 130.88 (s), 127.90 (s), 127.88

(s), 127.63 (s), 125.51 (s), 124.60 (s), 124.56 (s), 124.06 (s), 123.06 (s), 120.60 (s), 114.84 (s); HR-ESI-MS for $C_{18}H_{12}ON_5Cl_2$ ($[M+H]^+$) Calcd: 384.0419; Found: 384.0417.

4.2.11 Synthesis of N-(4-chloro-3-(8-chloro-[1,2,4]triazolo[4,3-a]pyridin-3-yl)phenyl)-3-(methylsulfonyl)benzamide (TPB10)

Thionyl chloride (0.356 g; 3 mmol) was added to a mixture of 3-(methylsulfonyl)benzoic acid (0.200 g, 1 mmol) in toluene and the mixture was heated at reflux for 3 hours. The reaction was cooled to room temperature and the solvent was removed under reduced pressure. The resultant acid chloride was dropwised to a mixture of **Compound 4** (0.279 g, 1 mmol) and DIPEA (0.258g, 2 mmol) in dichloromethane (15ml) at room temperature. The solution was stirred for overnight, then concentrated in vacuo. The residue was purified by silica gel column (DCM/MeOH=20/1) to afford **TPB10** (0.416 g, yield: 91%); purity: 98%; mp: 185.3-185.8°C; 1H -NMR (d6-DMSO): δ = 10.86 (s, 1H), 8.47 (t, J = 1.8 Hz, 1H), 8.35 – 8.23 (m, 1H), 8.17 – 8.04 (m, 4H), 7.81 (t, J = 7.8 Hz, 1H), 7.76 (d, J = 8.8 Hz, 1H), 7.67 (dd, J = 7.3, 0.8 Hz, 1H), 7.02 (t, J = 7.1 Hz, 1H), 3.27 (s, 3H); ^{13}C -NMR (d6-DMSO): δ = 164.74 (s), 147.95 (s), 146.07 (s), 141.64 (s), 138.79 (s), 135.77 (s), 133.21 (s), 130.97 (s), 130.62 (s), 130.34 (s), 127.98 (s), 127.89 (s), 126.59 (s), 125.67 (s), 124.78 (s), 124.61 (s), 124.09 (s), 120.62 (s), 114.85 (s), 43.88 (s); HR-ESI-MS for $C_{20}H_{13}O_3N_4Cl_2S$ ($[M-H]^+$) Calcd: 459.0085; Found: 459.0096.

4.2.12 Synthesis of 2-chloro-N-(4-chloro-3-(8-chloro-[1,2,4]triazolo[4,3-a]pyridin-3-yl)phenyl)-4-(methylsulfonyl)benzamide (TPB11)

Thionyl chloride (0.356 g; 3 mmol) was added to a mixture of 2-chloro-4-(methylsulfonyl)benzoic acid (0.235 g, 1 mmol) in toluene and the mixture

was heated at reflux for 3 hours. The reaction was cooled to room temperature and the solvent was removed under reduced pressure. The resultant acid chloride was dropwised to a mixture of Compound 4 (0.279 g, 1 mmol) and DIPEA (0.258g, 2 mmol) in dichloromethane (15ml) at room temperature. The solution was stirred for overnight, then concentrated in vacuo. The residue was purified by silica gel column (DCM/MeOH=20/1) to afford **TPB11** (0.432 g, yield: 88%); purity: 99%; mp: >290°C; ¹H-NMR (d6-DMSO): δ = 11.08 (s, 1H), 8.20 – 8.08 (m, 2H), 8.06 (d, J = 2.6 Hz, 1H), 7.99 (dd, J = 8.0, 1.7 Hz, 1H), 7.95 (dd, J = 8.8, 2.6 Hz, 1H), 7.90 (d, J = 8.0 Hz, 1H), 7.75 (d, J = 8.8 Hz, 1H), 7.70 – 7.63 (m, 1H), 7.02 (t, J = 7.1 Hz, 1H), 3.32 (s, 3H); ¹³C-NMR (d6-DMSO): δ = 164.48 (s), 147.97 (s), 146.04 (s), 143.68 (s), 141.08 (s), 138.43 (s), 131.38 (s), 131.17 (s), 130.41 (s), 128.58 (s), 128.19 (s), 127.90 (s), 126.41 (s), 125.96 (s), 124.14 (s), 123.96 (s), 123.81 (s), 120.59 (s), 114.82 (s), 43.52 (s); HR-ESI-MS for C₂₀H₁₂O₃N₄Cl₃S ([M-H]⁺) Calcd: 492.9696; Found: 492.9704.

4.2.13 synthesis of 2-chloro-N-(4-chloro-3-(8-chloro-[1,2,4]triazolo[4,3-a]pyridin-3-yl)phenyl)-4-fluorobenzamide (TPB12)

Thionyl chloride (0.356 g; 3 mmol) was added to a mixture of 2-chloro-4-fluorobenzoic acid (0.175 g, 1 mmol) in toluene and the mixture was heated at reflux for 3 hours. The reaction was cooled to room temperature and the solvent was removed under reduced pressure. The resultant acid chloride was dropwised to a mixture of Compound 4 (0.279 g, 1 mmol) and DIPEA (0.258g, 2 mmol) in dichloromethane (15ml) at room temperature. The solution was stirred for overnight, then concentrated in vacuo. The residue was purified by silica gel column (DCM/MeOH=20/1) to afford **TPB12** (0.280 g, yield: 65%); purity: 99%; mp: 237.5-239.2°C; ¹H-NMR (d6-DMSO): δ

= 10.95 (s, 1H), 8.19 – 8.13 (m, 1H), 8.11 (d, $J = 2.6$ Hz, 1H), 8.00 (dd, $J = 8.9, 2.6$ Hz, 1H), 7.81 – 7.73 (m, 2H), 7.73 – 7.68 (m, 1H), 7.63 (dd, $J = 9.0, 2.5$ Hz, 1H), 7.39 (d, $J = 2.5$ Hz, 1H), 7.06 (t, $J = 7.1$ Hz, 1H); ^{13}C -NMR (d6-DMSO): $\delta = 164.99$ (s), 164.12 (s), 161.63 (s), 148.00 (s), 146.14 (s), 138.78 (s), 133.54 (d, $J = 3.5$ Hz), 131.92 (d, $J = 11.0$ Hz), 131.36 (d, $J = 9.6$ Hz), 131.12 (s), 127.92 (d, $J = 3.8$ Hz), 125.89 (s), 124.18 (s), 123.84 (d, $J = 12.4$ Hz), 120.63 (s), 117.81 (s), 117.56 (s), 115.22 (s), 114.94 (d, $J = 14.1$ Hz); HR-ESI-MS for $\text{C}_{19}\text{H}_9\text{ON}_4\text{Cl}_3\text{F}$ ($[\text{M}-\text{H}]^+$) Calcd: 432.9826; Found: 432.9838.

4.2.14 Synthesis of 2-chloro-N-(4-chloro-3-(8-chloro-[1,2,4]triazolo[4,3-a]pyridin-3-yl)phenyl)-4-(trifluoromethyl)benzamide (TPB13)

Thionyl chloride (0.356 g; 3 mmol) was added to a mixture of 2-chloro-4-(trifluoromethyl)benzoic acid (0.224 g, 1 mmol) in toluene and the mixture was heated at reflux for 3 hours. The reaction was cooled to room temperature and the solvent was removed under reduced pressure. The resultant acid chloride was dropwised to a mixture of Compound 4 (0.279 g, 1 mmol) and DIPEA (0.258g, 2 mmol) in dichloromethane (15ml) at room temperature. The solution was stirred for overnight, then concentrated in vacuo. The residue was purified by silica gel column (DCM/MeOH=20/1) to afford **TPB13** (0.418 g, yield: 87%); purity: 98%; mp: 247.2-248.1°C; ^1H -NMR (d6-DMSO): $\delta = 11.08$ (s, 1H), 8.16 (d, $J = 6.9$ Hz, 1H), 8.14 – 8.05 (m, 2H), 7.99 (dd, $J = 8.9, 2.6$ Hz, 1H), 7.90 (s, 2H), 7.75 (dd, $J = 32.7, 8.0$ Hz, 2H), 7.06 (s, 1H); ^{13}C -NMR (d6-DMSO): $\delta = 164.61$ (s), 148.02 (s), 146.10 (s), 140.55 (s), 138.52 (s), 131.47 (s), 131.21 (s), 130.46 (s), 128.19 (s), 127.95 (s), 127.17 (d, $J = 3.4$ Hz), 127.11 (s), 125.99 (s), 124.95 (s), 124.89 (d, $J = 3.3$ Hz), 124.20 (s), 123.99 (s),

123.85 (s), 120.64 (s), 114.87 (s); HR-ESI-MS for $C_{20}H_9ON_4Cl_3F_3([M-H]^+)$ Calcd: 482.9794; Found: 482.9815.

4.2.15 Synthesis of N-(4-chloro-3-(8-chloro-[1,2,4]triazolo[4,3-a]pyridin-3-yl)phenyl)-2-fluoro-4-(trifluoromethyl)benzamide (TPB14)

Thionyl chloride (0.356 g; 3 mmol) was added to a mixture of 2-fluoro-4-(trifluoromethyl)benzoic acid (0.208 g, 1 mmol) in toluene and the mixture was heated at reflux for 3 hours. The reaction was cooled to room temperature and the solvent was removed under reduced pressure. The resultant acid chloride was dropwised to a mixture of Compound 4 (0.279 g, 1 mmol) and DIPEA (0.258g, 2 mmol) in dichloromethane (15ml) at room temperature. The solution was stirred for overnight, then concentrated in vacuo. The residue was purified by silica gel column (DCM/MeOH=20/1) to afford **TPB14** (0.321 g, yield: 69%); purity: 98%; mp:222.3-223.8°C; 1H -NMR (d6-DMSO): δ = 11.03 (s, 1H), 8.16 (dd, J = 6.9, 0.8 Hz, 1H), 8.12 (d, J = 2.6 Hz, 1H), 8.01 (dd, J = 8.9, 2.6 Hz, 1H), 7.98 – 7.88 (m, 2H), 7.78 (t, J = 8.3 Hz, 2H), 7.71 (dd, J = 7.2, 0.8 Hz, 1H), 7.06 (t, J = 7.1 Hz, 1H); ^{13}C -NMR (d6-DMSO): δ = 162.44 (s), 160.36 (s), 157.85 (s), 148.00 (s), 146.06 (s), 138.49 (s), 131.70 (d, J = 3.1 Hz), 131.18 (s), 128.95 (s), 128.79 (s), 128.19 (d, J = 3.4 Hz), 127.94 (s), 125.93 (s), 124.14 (d, J = 4.3 Hz), 123.98 (s), 122.24 – 122.01 (m), 120.64 (s), 114.87 (s), 114.61 (d, J = 3.8 Hz), 114.36 (d, J = 3.9 Hz); HR-ESI-MS for $C_{20}H_9ON_4Cl_2F_4([M-H]^+)$ Calcd: 467.0090; Found: 467.0105.

4.2.16 Synthesis of 2,6-dichloro-N-(4-chloro-3-(8-chloro-[1,2,4]triazolo[4,3-a]pyridine-3-yl)phenyl)nicotinamide (TPB15)

Thionyl chloride (0.356 g; 3 mmol) was added to a mixture of 2,6-dichloronicotinic acid (0.192 g, 1 mmol) in toluene and the mixture was heated at reflux for 3 hours. The reaction was cooled to room temperature and the solvent was removed under reduced pressure. The resultant acid chloride was dropwised to a mixture of Compound 4 (0.279 g, 1 mmol) and DIPEA (0.258g, 2 mmol) in dichloromethane (15ml) at room temperature. The solution was stirred for overnight, then concentrated in vacuo. The residue was purified by silica gel column (DCM/MeOH=20/1) to afford **TPB15** (0.340 g, yield: 76%); purity: 97%; mp: 138.9-139.7°C; ¹H-NMR (d6-DMSO): δ = 11.10 (s, 1H), 8.24 (d, J = 7.9 Hz, 1H), 8.20 – 8.12 (m, 1H), 8.08 (d, J = 2.6 Hz, 1H), 7.97 (dd, J = 8.9, 2.6 Hz, 1H), 7.78 (dd, J = 8.4, 5.3 Hz, 2H), 7.71 (dd, J = 7.2, 0.7 Hz, 1H), 7.06 (t, J = 7.1 Hz, 1H); ¹³C-NMR (d6-DMSO): δ = 163.46 (s), 150.28 (s), 148.02 (s), 146.31 (s), 146.07 (s), 141.89 (s), 138.43 (s), 132.21 (s), 131.24 (s), 128.30 (s), 127.95 (s), 126.02 (s), 124.29 (s), 124.20 (s), 124.00 (s), 123.84 (s), 120.64 (s), 114.87 (s); HR-ESI-MS for C₁₈H₉ON₅Cl₄ ([M-H]⁺) Calcd: 449.9484; Found: 449.9496.

4.2.17 Synthesis of 4-chloro-N-(4-chloro-3-(8-chloro-[1,2,4]triazolo[4,3-a]pyridin-3-yl)phenyl)-2-methylbenzamide (TPB16)

Thionyl chloride (0.356 g; 3 mmol) was added to a mixture of 4-chloro-2-methylbenzoic acid (0.171 g, 1 mmol) in toluene and the mixture was heated at reflux for 3 hours. The reaction was cooled to room temperature and the solvent was removed under reduced pressure. The resultant acid chloride was dropwised to a mixture of Compound 4 (0.279 g, 1 mmol) and DIPEA (0.258g, 2 mmol) in dichloromethane (15ml) at room temperature. The solution was stirred for overnight, then concentrated in vacuo. The residue was purified by silica gel column (DCM/MeOH=20/1) to afford

TPB16 (0.338 g, yield: 79%); purity: 99%; mp: 214.4-215.8°C; ¹H-NMR (d6-DMSO): δ = 10.76 (s, 1H), 8.21 – 8.10 (m, 2H), 8.01 (dd, J = 8.9, 2.6 Hz, 1H), 7.81 – 7.65 (m, 2H), 7.55 (d, J = 8.2 Hz, 1H), 7.48 – 7.37 (m, 2H), 7.06 (t, J = 7.1 Hz, 1H), 2.40 (s, 3H); ¹³C-NMR (d6-DMSO): δ = 167.61 (s), 147.99 (s), 146.18 (s), 139.06 (s), 138.71 (s), 135.72 (s), 134.90 (s), 131.00 (s), 130.77 (s), 129.69 (s), 127.93 (s), 127.64 (s), 126.14 (s), 125.75 (s), 124.15 (s), 124.00 (s), 123.90 (s), 120.65 (s), 114.88 (s), 19.56 (s); HR-ESI-MS for C₂₀H₁₂ON₄Cl₃ ([M-H]⁺) Calcd: 429.0077; Found: 429.0090.

4.2.18 Synthesis of 2-chloro-N-(4-chloro-3-(8-chloro-[1,2,4]triazolo[4,3-a]pyridin-3-yl)phenyl)-6-(trifluoromethyl)nicotinamide (TPB17)

Thionyl chloride (0.356 g; 3 mmol) was added to a mixture of 2-chloro-6-(trifluoromethyl)nicotinic acid (0.226 g, 1 mmol) in toluene and the mixture was heated at reflux for 3 hours. The reaction was cooled to room temperature and the solvent was removed under reduced pressure. The resultant acid chloride was dropwised to a mixture of Compound 4 (0.279 g, 1 mmol) and DIPEA (0.258g, 2 mmol) in dichloromethane (15ml) at room temperature. The solution was stirred for overnight, then concentrated in vacuo. The residue was purified by silica gel column (DCM/MeOH=20/1) to afford **TPB17** (0.295 g, yield: 61%); purity: 97%; mp: 149.6-150.5°C; ¹H-NMR (d6-DMSO): δ = 11.19 (s, 1H), 8.48 (d, J = 7.8 Hz, 1H), 8.22 – 8.12 (m, 2H), 8.09 (d, J = 2.6 Hz, 1H), 7.98 (dd, J = 8.9, 2.6 Hz, 1H), 7.81 (d, J = 8.9 Hz, 1H), 7.71 (dd, J = 7.2, 0.8 Hz, 1H), 7.06 (t, J = 7.1 Hz, 1H); ¹³C-NMR (d6-DMSO): δ = 163.20 (s), 148.03 (s), 147.61 (s), 147.44 (s), 146.05 (s), 141.18 (s), 138.29 (s), 136.45 (s), 131.30 (s), 128.47 (s), 127.96 (s), 126.09 (s), 124.21 (s), 124.05 (s), 123.88 (s),

122.31 (s), 121.08 (d, $J = 2.4$ Hz), 120.64 (s), 114.87 (s); HR-ESI-MS for $C_{19}H_{10}ON_5Cl_3F_3$ ($[M+H]^+$) Calcd: 485.9903; Found: 485.9891.

4.2.19 Synthesis of 2-chloro-N-(4-chloro-3-(8-chloro-[1,2,4]triazolo[4,3-a]pyridin-3-yl)phenyl)-6-fluorobenzamide (TPB18)

Thionyl chloride (0.356 g; 3 mmol) was added to a mixture of 2-chloro-6-fluorobenzoic acid (0.175 g, 1 mmol) in toluene and the mixture was heated at reflux for 3 hours. The reaction was cooled to room temperature and the solvent was removed under reduced pressure. The resultant acid chloride was dropwised to a mixture of Compound 4 (0.279 g, 1 mmol) and DIPEA (0.258g, 2 mmol) in dichloromethane (15ml) at room temperature. The solution was stirred for overnight, then concentrated in vacuo. The residue was purified by silica gel column (DCM/MeOH=20/1) to afford **TPB18** (0.370 g, yield: 86%); purity: 97%; mp: 200.4-201.6°C; 1H -NMR (d6-DMSO): $\delta = 11.25$ (s, 1H), 8.18 (d, $J = 6.9$ Hz, 1H), 8.10 (d, $J = 2.5$ Hz, 1H), 7.98 (dd, $J = 8.9, 2.6$ Hz, 1H), 7.78 (d, $J = 8.8$ Hz, 1H), 7.70 (d, $J = 7.2$ Hz, 1H), 7.58 (dd, $J = 8.5, 6.0$ Hz, 1H), 7.49 (d, $J = 8.1$ Hz, 1H), 7.42 (t, $J = 8.6$ Hz, 1H), 7.06 (t, $J = 7.1$ Hz, 1H); ^{13}C -NMR (d6-DMSO): $\delta = 160.99$ (s), 160.39 (s), 157.92 (s), 148.02 (s), 146.10 (s), 138.38 (s), 132.64 (d, $J = 9.2$ Hz), 131.48 (d, $J = 5.6$ Hz), 131.28 (s), 128.28 (s), 127.94 (s), 126.10 (dd, $J = 13.1, 7.1$ Hz), 125.75 (s), 124.28 (s), 123.73 (d, $J = 16.4$ Hz), 120.61 (s), 115.53 (s), 115.32 (s), 114.82 (s); HR-ESI-MS for $C_{19}H_9ON_4Cl_3F$ ($[M-H]^+$) Calcd: 432.9826; Found: 432.9833.

4.2.20 synthesis of 2-chloro-N-(4-chloro-3-(8-chloro-[1,2,4]triazolo[4,3-a]pyridin-3-yl)phenyl)nicotinamide (TPB19)

Thionyl chloride (0.356 g; 3 mmol) was added to a mixture of 2-chloronicotinic acid (0.158 g, 1 mmol) in toluene and the mixture was heated at reflux for 3 hours. The reaction was cooled to room temperature and the solvent was removed under reduced pressure. The resultant acid chloride was dropwised to a mixture of Compound 4 (0.279 g, 1 mmol) and DIPEA (0.258g, 2 mmol) in dichloromethane (15ml) at room temperature. The solution was stirred for overnight, then concentrated in vacuo. The residue was purified by silica gel column (DCM/MeOH=20/1) to afford **TPB19** (0.244 g, yield: 59%); purity: 99%; mp: 242.1-243.4°C; ¹H-NMR (d6-DMSO): δ = 11.08 (s, 1H), 8.57 (dd, J = 4.9, 1.9 Hz, 1H), 8.15 (ddd, J = 9.5, 7.3, 1.4 Hz, 2H), 8.11 (d, J = 2.6 Hz, 1H), 7.99 (dd, J = 8.8, 2.6 Hz, 1H), 7.79 (d, J = 8.8 Hz, 1H), 7.71 (dd, J = 7.3, 0.9 Hz, 1H), 7.60 (dd, J = 7.6, 4.8 Hz, 1H), 7.06 (t, J = 7.1 Hz, 1H); ¹³C-NMR (d6-DMSO): δ = 164.41 (s), 151.32 (s), 148.02 (s), 146.86 (s), 146.11 (s), 138.79 (s), 138.62 (s), 133.13 (s), 131.21 (s), 128.14 (s), 127.95 (s), 125.98 (s), 124.20 (s), 123.93 (s), 123.79 (s), 123.74 (s), 120.64 (s), 114.87 (s); HR-ESI-MS for C₁₈H₉ON₅Cl₃ ([M-H]⁺) Calcd: 415.9873; Found: 415.9881.

4.2.21 synthesis of N-(4-chloro-3-(8-chloro-[1,2,4]triazolo[4,3-a]pyridin-3-yl)phenyl)isoxazole-3-carboxamide (TPB20)

Thionyl chloride (0.356 g; 3 mmol) was added to a mixture of isoxazole-3-carboxylic acid (0.113 g, 1 mmol) in toluene and the mixture was heated at reflux for 3 hours. The reaction was cooled to room temperature and the solvent was removed under reduced pressure. The resultant acid chloride was dropwised to a mixture of Compound 4 (0.279 g, 1 mmol) and DIPEA (0.258g, 2 mmol) in dichloromethane (15ml) at room temperature. The solution was stirred for overnight, then concentrated in

vacuo. The residue was purified by silica gel column (DCM/MeOH=20/1) to afford **TPB20** (0.268 g, yield: 72%); purity: 98%; mp: 233.8-234.9°C; $^1\text{H-NMR}$ (d₆-DMSO): δ = 11.16 (s, 1H), 9.20 (d, J = 1.7 Hz, 1H), 8.20 (d, J = 2.6 Hz, 1H), 8.17 (dd, J = 7.0, 0.8 Hz, 1H), 8.12 (dd, J = 8.9, 2.6 Hz, 1H), 7.79 (d, J = 8.8 Hz, 1H), 7.71 (dd, J = 7.2, 0.8 Hz, 1H), 7.12 – 7.01 (m, 2H); $^{13}\text{C-NMR}$ (d₆-DMSO): δ = 162.43 (s), 158.45 (s), 158.02 (s), 147.99 (s), 146.00 (s), 138.09 (s), 131.09 (s), 128.51 (s), 127.96 (s), 125.73 (s), 124.79 (s), 124.74 (s), 124.14 (s), 120.65 (s), 114.90 (s), 105.13 (s); HR-ESI-MS for $\text{C}_{16}\text{H}_8\text{O}_2\text{N}_5\text{Cl}_2$ ($[\text{M-H}]^+$) Calcd: 372.0055; Found: 372.0064.

4.3. Biology

4.3.1. Cultured cells

The following cell lines were obtained from Cobioer (Cobioer Biosciences Co., Ltd., Nanjing, China): MDA-MB-231, MDA-MB-468, MCF-7, T47D, A549, U251, AN3-CA, Hela, NIH3T3 and MCF-10A. Cell were tested for mycoplasma by the MycoAlert Mycoplasma Detection Kit (LONZA, USA). All reagents were purchased from Sigma-Aldrich or Gibco. The MDA-MB-231, MDA-MB-468, MCF-7, T47D, A549, U251, AN3-CA, Hela cell lines were maintained in RPMI 1640 medium supplemented with 10% fetal bovine serum (FBS), while the NIH3T3 cell line was maintained in DMEM medium supplemented with 10% FBS. MCF10A cells were cultured in DMEM/F12 with 5% horse serum, 20 ng/ml epidermal growth factor, 0.5 ug/ml hydrocortisone, 10 ug/ml insulin, 100 ng/ml cholera toxin³⁵. All cells were grown in a humidified atmosphere with 5% CO₂ at 37°C.

4.3.2. Gli-Luciferase Reporter Assay

The effect of the compounds on Gli1-promoter activated luciferase activity was examined in NIH3T3 cells using the Dual-Luciferase Assay system (Promega, Madison, WI), according to the manufacturer's instructions. Cells were co-transfected with the 8 × 3' Gli-BS-delta51-Luc II reporter plasmid³⁶ (Sangon Biotech Co., Ltd., Shanghai, China) and pRL-TK, Renilla reporter (Sangon Biotech Co.). After 24 h, cells were treated with our compounds and SAG, a Hh signaling pathway activator. Relative values of Gli1 luciferase signal was calculated by normalization to Renilla luciferase values, and the results were expressed as the compound concentration necessary to inhibit 50% of the normalized luciferase activity.

4.3.3. *Cell proliferation assay in vitro*

The antiproliferative activity of compound **TPB1-TPB20** against MDA-MB-468, MDA-MB-231, MCF-7, T47D, A549, U251, AN3-CA, MCF-10A and Hela cell lines was evaluated in vitro by MTT assay. All cells were plated in 96-well plates overnight. Our compounds were added to the wells at various concentrations. After 72 h, MTT was added for another 4 h, and the absorbance was measured at 570 nm. The inhibition rate is calculated as follows: $\text{Inhibition\%} = [(\text{control} - \text{compound}) / (\text{control} - \text{blank})] \times 100\%$, **VIS** was used as a reference drug and tested under similar conditions. The IC₅₀ values were determined with the Prism statistical package (GraphPad Software, San Diego, CA, U.S.A.)

4.3.4. *5-Ethynyl-20-deoxyuridine assay*

Based on manufacturer's instruction, the cells were treated with 5-ethynyl-20-deoxyuridine (RiboBio, Guangzhou, China) for 5 h. After washing three times with PBS, cells were incubated with Apollo reaction cocktail and stained with

Hoechst 33342. The cell proliferation activity was evaluated by the ratio of EDU-stained cells (red fluorescence) to Hoechst-stained cells (blue fluorescence)³⁷. The intensity of the fluorescence was quantified by the ImageJ (National Institutes of Health, U.S.A.).

4.3.5. *Cell apoptosis and cycle assay*

MDA-MB-468 and MDA-MB-231 cells (1.2×10^5 cells/well in 6-well plates) were treated with different concentrations of **TPB15** for 48 h. The cells were stained by PI and Annexin V-FITC. For the cell cycle assay, the cell suspension was collected and fixed with 75% ethanol at -20°C overnight followed by staining with PI. Cell apoptosis and cycle distribution were measured by the FACS Calibur flow cytometer (Becton Dickinson, San Jose, CA, USA).

4.3.6. *Immunoblot analysis*

Immunoblot analysis was conducted as described previously³⁸. The primary antibodies were used, including Smo (Abcam, ab72130, USA), Ptch2 (CST, 2464S, USA), Shh (CST, 2207S, USA), Gli1 (CST, 3538S, USA), GAPDH (CST, 2118S, USA), Bax (CST, 5023S, USA), Bcl-2 (CST, 4223S, USA). After TBST washes, the membranes were incubated with corresponding horseradish peroxidase-conjugated secondary antibodies (Bio-Rad) for 1 h at room temperature. Each experiment was performed in triplicate.

4.3.7. *qRT-PCR analysis*

On the basis of manufacturer's instructions, total RNA was extracted with RNAiso Plus Kit (TaKaRa, Dalian, China) and reverse-transcribed to cDNA with a SuperScript III Kit (TaKaRa). The mRNA expression levels were measured three times with an SYBR Green Kit (TaKaRa) in a LightCycle 480 system (Roche, Basel, Switzerland). The

expression of genes was normalized to GAPDH mRNA expression. The primer sequences were shown in supporting information (**Table S1**).

4.3.8. *Molecular modeling studies*

The Induce-fit docking (IFD) method from Schrodinger2017-1 (maestro11.1) was used to elucidate the binding model of potent compounds ²⁶. The complex structure **VIS** was retrieved from the RCSB database (PDB entry: 5L7I²⁷). The key residues Asp384, Arg400, Gln477, Phe484, Tyr394 were selected as grid box for binding site ²⁸.

Screenshots of the docking structures were visualized using PyMOL 1.3.X.

4.3.9. *Surface plasmon resonance (SPR) analysis*

The analyses of interactions between Smo protein (Abnova, H00006608-G01, Taiwan) and our compounds was performed in PBS and a flow rate of 2 μ L/s at 4°C. Compounds were injected at different concentrations (2.5, 5, 10 μ M) to determine their rate constants. The sensor chip surface was regenerated by injection of 0.5 % SDS: Glycine-HCL (pH=2.0) =1:1 solution. The data is monitored in real time on the plexera SPRi system. Kinetic analysis of sensorgram data and kinetic constants were calculated from the sensorgrams with BIA evaluation41 (BIAcore) according to the global fitting model.

4.3.10. *Fluorescence binding assays*

HEK293 cells were transiently transfected with a plasmid that encodes Smo-WT (Sangon Biotech Co., Ltd., Shanghai, China). On the basis of manufacturer' instructions, the transfection was done in triplicate using Lipofectamine 2000 (Invitrogen). The transfection was verified by western blot (**Fig. 4A**). The transfected cells were divided into 4 groups: BODIPY-cyclopamine group, cyclopamine group (25 μ M cyclopamine),

TPB15 group (1 μ M or 25 μ M **TPB15**). All groups were treated with BODIPY-cyclopamine and then treated with corresponding compounds. All groups were incubated 37 °C for 12 h, and cells were incubated with Hoechst 33342. Images were taken with the inverted fluorescence microscope (Axio observer, Carl Zeiss, Oberkochen, Germany) for further analysis.

4.3.11. Immunofluorescence staining

NIH3T3 cells were seeded at 2×10^4 cells/well on chamber glass slides in 24-well plates at 37°C for 24 h, and then treated with the SAG (Hedgehog pathway activator, 200 nM) for 6 h. Cells were incubated with various compounds for 24 h. Samples were fixed with 4% paraformaldehyde, permeated by 0.1% triton, and stained with antibodies against Ac-Tub (#5335, Cell Signaling Technology) and Smo (#72130, Abcam). FITC AffiniPure (Earthox, E031220-01, USA) and Alexa Fluor 555 (Cell Signaling Technology, #8953, USA) were used as the secondary antibody. Images were taken with the Inverted confocal laser microscope (LSM 880 with Airyscan, Carl Zeiss, Oberkochen, Germany).

4.3.12. Acute toxicity test

LD₅₀ is used to evaluate the toxicity of drugs using Kunming mice. Animal experimental procedures comply with the Care and Use of Laboratory Animals Guide and approved by the Animal Experimental Ethics Committee of Southern Medical University. In this study, improved Karber's method was used to determine the LD₅₀³². Compounds were administered by gavage at various concentrations and mice were observed over 14 days to record the mortality. The LD₅₀ was calculated as follows:

$$LD_{50} = lg^{-1}[x_m - i(\sum P - 0.5)]$$

X_m is the logarithm of the maximal dose; P the mortality for each group; $\sum P$ is the summation of the mortalities; i is the logarithm of the ratio between the neighboring two dose group (high dose and low dose).

4.3.13. *In vivo anti-tumor evaluation*

Female BALB/c nude mice, 6 to 8 weeks old, were purchased from Guangdong Medical Animal Experimental Center (Guangdong, China). Animal experimental procedures comply with the Care and Use of Laboratory Animals Guide and approved by the Animal Experimental Ethics Committee of Southern Medical University. MDA-MB-468 cells (1.0×10^7 in 0.2 ml PBS) were subcutaneously injected into the right side of the posterior flanks of nude mice. When tumor volumes reached 100 mm³, mice were randomly divided into three groups of five mice. The **TPB15** group treated with 80 mg/kg given by gavage every day in a vehicle of saline with 0.1% Tween 80. The **VIS** group received 100 mg/kg every day in the same vehicle through intragastric administration. The control group received vehicle everyday via intragastric administration. Body weight was recorded every day and tumor volumes were measured every 2 days. At day 21, mice were sacrificed and tumors were excised and weighed.

Declaration of Competing interest

All authors declare that they have no known competing financial interests or personal relationships that could have appeared to influence the work reported in this paper.

Acknowledge

This work was supported by the Natural Science Foundation of Guangdong Province, China (No. 2018A030313405), the Science and Technology Planning Project of Guangdong Province, China (No. 2017A050501020) and the Medical Scientific Research Foundation of Guangdong Province, China (No. A2018189).

Appendix A. Supplementary data

Supplementary data associated with this article can be found, in the online version.

References

1. Scales, S. J.; de Sauvage, F. J. *Trends Pharmacol Sci* **2009**, *30*, 303.
2. Liu, G.; Xue, D.; Yang, J., et al. *Journal of medicinal chemistry* **2016**, *59*, 11050.
3. Corbit, K. C.; Aanstad, P.; Singla, V., et al. *Nature* **2005**, *437*, 1018.
4. Pietrobono, S.; Stecca, B. *Cells* **2018**, *7*.
5. Briscoe, J.; Therond, P. P. *Nature reviews. Molecular cell biology* **2013**, *14*, 416.
6. Yang, L.; Xie, G.; Fan, Q., et al. *Oncogene* **2010**, *29*, 469.
7. Xin, M. H.; Ji, X. Y.; De La Cruz, L. K., et al. *Med Res Rev* **2018**, *38*, 870.
8. Infante, P.; Alfonsi, R.; Botta, B., et al. *Trends Pharmacol Sci* **2015**, *36*, 547.
9. Ma, H.; Li, H. Q.; Zhang, X. *Current topics in medicinal chemistry* **2013**, *13*, 2208.
10. Rimkus, T. K.; Carpenter, R. L.; Qasem, S., et al. *Cancers* **2016**, *8*.
11. Silapunt, S.; Chen, L.; Migden, M. R. *Ther Adv Med Oncol* **2016**, *8*, 375.
12. Kucukyurt, S.; Eskazan, A. E. *British journal of clinical pharmacology* **2019**.
13. Erdem, G. U.; Sendur, M. A. N.; Ozdemir, N. Y., et al. *Curr Med Res Opin* **2015**, *31*, 743.
14. Burness, C. B.; Scott, L. J. *Target Oncol* **2016**, *11*, 239.
15. O'Toole, S. A.; Machalek, D. A.; Shearer, R. F., et al. *Cancer research* **2011**, *71*, 4002.
16. Huang, Y. J.; Fang, J. S.; Lu, W. Q., et al. *Cell Chem Biol* **2019**, *26*, 1143.
17. Sun, M. J.; Zhang, N.; Wang, X. L., et al. *Cell Biosci* **2016**, *6*.
18. Maubant, S.; Tesson, B.; Maire, V., et al. *PloS one* **2015**, *10*.
19. Ruiz-Borrego, M.; Jimenez, B.; Antolin, S., et al. *Invest New Drug* **2019**, *37*, 98.
20. Cazet, A. S.; Hui, M. N.; Elsworth, B. L., et al. *Nat Commun* **2018**, *9*.
21. Zhang, X. J.; Zhao, F.; Wu, Y. R., et al. *Nat Commun* **2017**, *8*.
22. Rotzinger, S.; Bourin, M.; Akimoto, Y., et al. *Cellular and molecular neurobiology* **1999**, *19*, 427.
23. East, S. P.; White, C. B.; Barker, O., et al. *Bioorganic & medicinal chemistry letters* **2009**, *19*, 894.
24. Bao, X.; Peng, Y.; Lu, X., et al. *Bioorganic & medicinal chemistry letters* **2016**, *26*, 3048.
25. Benvenuto, M.; Masuelli, L.; De Smaele, E., et al. *Oncotarget* **2016**, *7*, 9250.
26. Wang, C. L.; Zhu, M. F.; Lu, X. H., et al. *Bioorgan Med Chem* **2018**, *26*, 3308.
27. Byrne, E. F. X.; Sircar, R.; Miller, P. S., et al. *Nature* **2016**, *535*, 517.
28. Lu, W. F.; Zhang, D. H.; Ma, H. K., et al. *European journal of medicinal chemistry* **2018**, *155*, 34.
29. Chen, J. K.; Taipale, J.; Cooper, M. K., et al. *Genes Dev* **2002**, *16*, 2743.
30. Corbit, K. C.; Aanstad, P.; Singla, V., et al. *Nature* **2005**, *437*, 1018.
31. Xu, X.; Su, B.; Xie, C., et al. *PloS one* **2014**, *9*, e96441.
32. Wang, J.; Sun, F.; Tang, S., et al. *Regulatory toxicology and pharmacology : RTP* **2017**, *86*, 49.
33. Bray, F.; Ferlay, J.; Soerjomataram, I., et al. *Ca-Cancer J Clin* **2018**, *68*, 394.
34. Hwang, S. Y.; Park, S.; Kwon, Y. *Pharmacol Therapeut* **2019**, *199*, 30.
35. Wang, M.; Ning, X.; Chen, A., et al. *Scientific reports* **2015**, *5*, 12223.
36. Han, B.; Qu, Y.; Jin, Y., et al. *Cell reports* **2015**, *13*, 1046.
37. Xiong T, H. C., Li J, Yu S, Chen F, Zhang Z, Zhuang C, Li Y, Zhuang C, Huang X, Ye J, Zhang F, Gui Y. *J Cancer* **2020**, *11*, 1751.
38. Wu, S. Y.; Chen, T. M.; Gmeiner, W. H., et al. *Nucleic Acids Res* **2013**, *41*, 4650.

Abstract:

Triple-negative breast cancer (TNBC), a subset of breast cancers, have poorer survival than other breast cancer types. Recent studies have demonstrated that the abnormal Hedgehog (Hh) pathway is activated in TNBC and that these treatment-resistant cancers are sensitive to inhibition of the Hh pathway. Smoothed (Smo) protein is a vital constituent in Hh signaling and an attractive drug target. Vismodegib (**VIS**) is one of the most widely studied Smo inhibitors. But the clinical application of Smo inhibitors is limited to adult patients with BCC and AML, with many side effects. Therefore, it's necessary to develop novel Smo inhibitor with better profiles. Twenty [1,2,4]triazolo[4,3-a]pyridines were designed, synthesized and screened as Smo inhibitors. Four of these novel compounds showed directly bound to Smo protein with stronger binding affinity than **VIS**. The new compounds showed broad anti-proliferative activity against cancer cell lines in vitro, especially triple-negative breast cancer cells. Mechanistic studies demonstrated that **TPB15** markedly induced cell cycle arrest and apoptosis in MDA-MB-468 cells. **TPB15** blocked Smo translocation into the cilia and reduced Smo protein and mRNA expression. Furthermore, the expression of the downstream regulatory factor glioma-associated oncogene 1 (Gli1) was significantly inhibited. Finally, **TPB15** demonstrated greater anti-tumor activity in our animal models than **VIS** with lower toxicity. Hence, these results support further optimization of this novel scaffold to develop improved Smo antagonists.

Declaration of interests

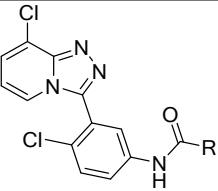
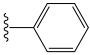
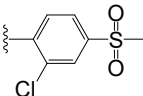
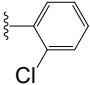
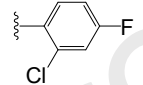
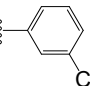
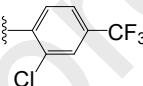
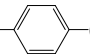
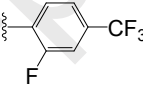
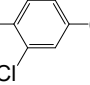
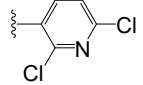
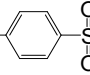
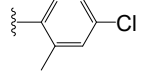
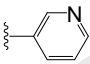
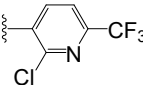
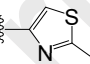
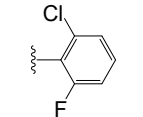
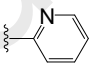
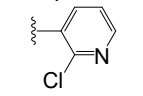
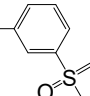
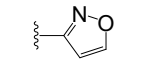
☒ The authors declare that they have no known competing financial interests or personal relationships that could have appeared to influence the work reported in this paper.

☐ The authors declare the following financial interests/personal relationships which may be considered as potential competing interests:

Highlights

- A series of 8-chloro-[1,2,4]triazolo[4,3-a]pyridine derivatives were designed and synthesized.
- Compounds **TPB3**、**TPB14**、**TPB15** and **TPB17** showed significant inhibition of Hedgehog pathway activation ($IC_{50} < 0.100 \mu M$).
- **TPB15** not only suppressed Hh signaling by blocking Smo translocation into the cilia but also reduced the expression of Smo.
- **TPB15** demonstrated greater anti-tumor activity in our animal models than Vismodegib with significantly lower toxicity.

Table 1. Chemical structures and activity of compounds (TPB1-TPB20).

					
Compd	R	IC ₅₀ of Gli-luc reporter (μM)	Compd	R	IC ₅₀ of Gli-luc reporter (μM)
TPB1		0.770 ± 0.070	TPB11		4.274 ± 0.222
TPB2		0.727 ± 0.145	TPB12		8.218 ± 0.457
TPB3		0.102 ± 0.020	TPB13		5.204 ± 0.381
TPB4		2.725 ± 0.334	TPB14		0.096 ± 0.002
TPB5		0.285.5 ± 0.020	TPB15		0.090 ± 0.007
TPB6		1.767 ± 0.307	TPB16		> 10
TPB7		> 10	TPB17		0.093 ± 0.013
TPB8		> 10	TPB18		> 10
TPB9		1.079 ± 0.107	TPB19		> 10
TPB10		2.979 ± 0.299	TPB20		> 10
VIS		0.1000 ± 0.022			

^aIC₅₀ denote the drug concentration that inhibits 50% of Gli-luc reporter. Values represent the mean ± S.D. from 3–5 separate experiments.

Table 2. Anti-proliferative effects of compounds (TPB1-TPB20).

Compd	IC ₅₀ (μM)								
	MDA-MB -468	MDA-MB -231	MCF-7	T47D	A549	U251	AN3-CA	Hela	MCF10A
TPB1	>100	58.2 ± 2.0	>100	>100	76.9 ± 7.4	73.5 ± 7.1	67.6 ± 7.9	>100	
TPB2	>100	59.9 ± 1.6	92.2 ± 6.9	83.8 ± 2.6	>100	>100	>100	>100	
TPB3	54.8 ± 5.5	66.1 ± 9.1	71.9 ± 16.9	30.2 ± 5.3	52.7 ± 1.7	43.1 ± 9.6	68.4 ± 8.7	>100	
TPB4	>100	>100	58.4 ± 8.1	>100	73.6 ± 7.5	>100	>100	>100	
TPB5	21.6 ± 0.9	>100	78.2 ± 6.0	>100	61.3 ± 12.4	>100	84.8 ± 19.0	>100	
TPB6	>100	>100	94.2 ± 3.9	>100	>100	>100	>100	>100	
TPB7	>100	>100	>100	>100	>100	>100	>100	>100	
TPB8	>100	>100	>100	>100	>100	74.3 ± 1.5	>100	79.8 ± 6.5	
TPB9	>100	92.0 ± 4.4	96.4 ± 11.2	>100	>100	79.0 ± 19.4	>100	75.5 ± 15.5	
TPB10	>100	>100	88.9 ± 10.2	>100	>100	>100	>100	86.4 ± 7.7	
TPB11	>100	37.2 ± 1.3	>100	>100	>100	44.6 ± 5.6	>100	>100	
TPB12	>100	75.0 ± 2.4	>100	>100	>100	>100	>100	>100	
TPB13	>100	>100	81.6 ± 19.7	>100	>100	>100	>100	>100	
TPB14	22.3 ± 1.1	>100	62.8 ± 7.6	70.8 ± 6.8	>100	>100	41.2 ± 12.5	61.9 ± 16.1	
TPB15	28.6 ± 3.2	29.5 ± 3.2	61.5 ± 4.4	42.3 ± 8.2	64.9 ± 37.5	85.2 ± 3.9	44.5 ± 9.8	66.3 ± 14.6	>100
TPB16	34.3 ± 4.8	>100	>100	>100	>100	>100	>100	>100	
TPB17	46.0 ± 7.9	>100	>100	87.6 ± 32.1	46.8 ± 22.3	>100	48.3 ± 7.0	86.3 ± 20.0	
TPB18	57.6 ± 10.1	>100	>100	>100	72.3 ± 2.7	>100	>100	>100	
TPB19	>100	89.7 ± 5.2	>100	>100	35.8 ± 8.1	>100	>100	87.5 ± 25.8	
TPB20	>100	>100	>100	>100	42.7 ± 6.5	>100	>100	>100	
VIS	79 ± 3.2	>100	>100	>100	>100	>100	93 ± 4.5	61.7 ± 7.6	89.5 ± 12.3

^aIC₅₀ denote the drug concentration that inhibits 50% of cell growth. Values represent the mean ± S.D. from 3–5 separate experiments.

Table 3. The binding strength of TPB3, TPB14, TPB15, TPB17 and VIS to the Smo receptor

Cmpd	ka ^a (1/Ms)	kd ^b (1/s)	Rmax ^c (RU)	KA ^d (1/M)	KD ^e (M)
TPB3	101	1.23×10 ⁻³	41.2	8.21×10 ⁴	1.21×10 ⁻⁵
TPB14	111	1.51×10 ⁻³	49.2	7.35×10 ⁴	1.36×10 ⁻⁵
TPB15	360	3.75×10 ⁻⁶	90.5	9.71×10 ⁷	1.03×10 ⁻⁸
TPB17	260	2.75×10 ⁻⁶	8.44	9.43×10 ⁷	1.06×10 ⁻⁸
VIS	179	1.74×10 ⁻⁵	4.63	1.03×10 ⁷	9.75×10 ⁻⁸

^a ka = association rate constant

^b kd = dissociation rate constant

^c Rmax = maximum resonance response at equilibrium

^d KA = the equilibrium association constant

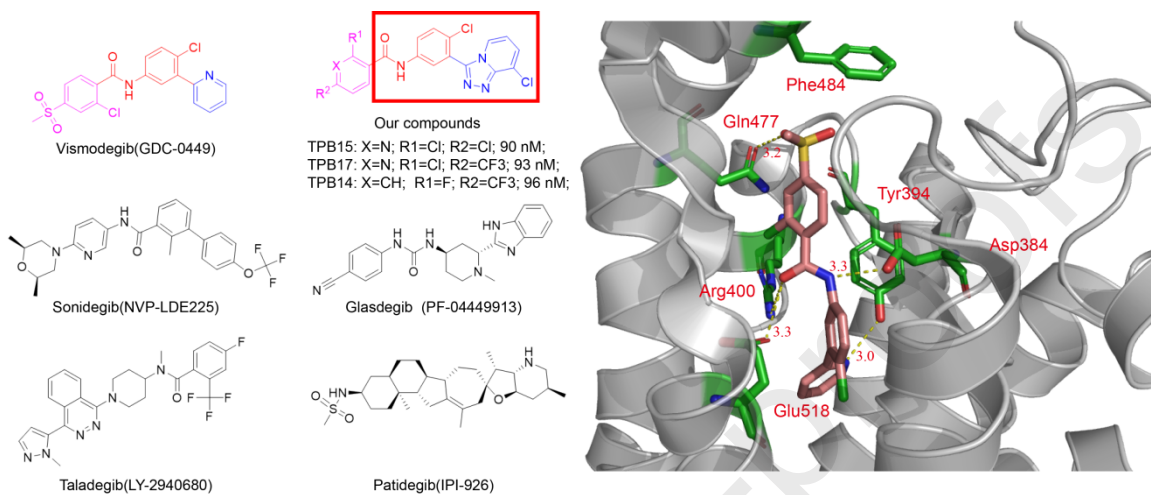
^e KD = the equilibrium dissociation constant

Table 4. Acute toxicity of TPB3, TPB15 and VIS

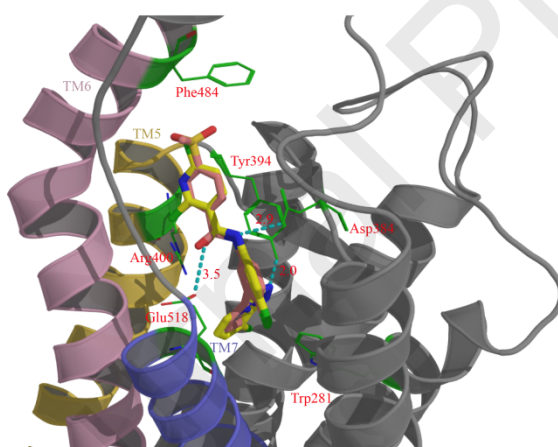
Cmpd	Dose (mg/kg)	Mortality (D/T)		Mortality (%)	LD ₅₀ (mg/kg)
		Female	Male		
TPB3	5000	0/5	0/5	0	> 5000
	3008	1/5	0/5	10	
	3453	2/5	1/5	30	
TPB15	3965	3/5	2/5	50	3875
	4552	3/5	3/5	60	
	5226	4/5	3/5	70	
	741	1/5	0/5	10	
	1111	1/5	2/5	30	
VIS	1778	3/5	2/5	50	2008
	2667	4/5	2/5	60	
	4000	4/5	4/5	80	

D/T: dead/treated mice. 95% confidence intervals of TPB15 were between 2807 and 4956

mg/kg. 95% confidence intervals of **VIS** were between 788 and 3623 mg/kg.



A



B

